

This discussion paper is/has been under review for the journal Biogeosciences (BG).
Please refer to the corresponding final paper in BG if available.

Icehouse-greenhouse variations in marine denitrification

T. J. Algeo¹, P. A. Meyers², R. S. Robinson³, H. Rowe⁴, and G. Q. Jiang⁵

¹Department of Geology, University of Cincinnati, Cincinnati, Ohio 45221-0013, USA

²Department of Earth and Environmental Sciences, University of Michigan, Ann Arbor, Michigan 48109-1005, USA

³Graduate School of Oceanography, University of Rhode Island, Narragansett, RI 02882, USA

⁴Bureau of Economic Geology, University of Texas at Austin, Austin, Texas 78713-8924, USA

⁵Department of Geoscience, University of Nevada at Las Vegas, Las Vegas, NV 89154-4010, USA

Received: 12 August 2013 – Accepted: 19 August 2013 – Published: 6 September 2013

Correspondence to: T. J. Algeo (thomas.algeo@uc.edu)

Published by Copernicus Publications on behalf of the European Geosciences Union.

BGD

10, 14769–14813, 2013

Icehouse-greenhouse variations in marine denitrification

T. J. Algeo et al.

Title Page

Abstract

Introduction

Conclusions

References

Tables

Figures

◀

▶

◀

▶

Back

Close

Full Screen / Esc

Printer-friendly Version

Interactive Discussion



Abstract

Long-term secular variation in the isotopic composition of seawater fixed nitrogen (N) is poorly known. Here, we document variation in the N-isotopic composition of marine sediments ($\delta^{15}\text{N}_{\text{sed}}$) since 660 Ma (million years ago) in order to understand major changes in the marine N cycle through time and their relationship to first-order climate variation. During the Phanerozoic, greenhouse climate modes were characterized by low $\delta^{15}\text{N}_{\text{sed}}$ (~ -2 to $+2$ ‰) and icehouse climate modes by high $\delta^{15}\text{N}_{\text{sed}}$ ($\sim +4$ to $+8$ ‰). Shifts toward higher $\delta^{15}\text{N}_{\text{sed}}$ occurred rapidly during the early stages of icehouse modes, prior to the development of major continental glaciation, suggesting a potentially important role for the marine N cycle in long-term climate change. Reservoir box modeling of the marine N cycle demonstrates that secular variation in $\delta^{15}\text{N}_{\text{sed}}$ was likely due to changes in the dominant locus of denitrification, with a shift in favor of sedimentary denitrification during greenhouse modes owing to higher eustatic (global sea-level) elevations and greater on-shelf burial of organic matter, and a shift in favor of water-column denitrification during icehouse modes owing to lower eustatic elevations, enhanced organic carbon sinking fluxes, and expanded oceanic oxygen-minimum zones. The results of this study provide new insights into operation of the marine N cycle, its relationship to the global carbon cycle, and its potential role in modulating climate change at multimillion-year timescales.

1 Introduction

Nitrogen (N) plays a key role in marine productivity and organic carbon fluxes and is thus a potentially major influence on the global climate system (Gruber and Galloyay, 2008). Variation in marine sediment N-isotopic compositions during the Quaternary (2.6 Ma to the present) has been linked to changes in organic carbon burial and oceanic denitrification rates during Pleistocene glacial-interglacial cycles (François et al., 1992; Altabet et al., 1995; Ganeshram et al., 1995; Haug et al., 1998; Naqvi et al.,

BGD

10, 14769–14813, 2013

Icehouse-greenhouse variations in marine denitrification

T. J. Algeo et al.

Title Page

Abstract

Introduction

Conclusions

References

Tables

Figures

◀

▶

◀

▶

Back

Close

Full Screen / Esc

Printer-friendly Version

Interactive Discussion



1998; Broecker and Henderson, 1998; Suthhof et al., 2001; Liu et al., 2005; 2008). At this timescale (i.e., $\sim 10^5$ yr), the marine N cycle is thought to act mainly as a positive climate feedback, but negative feedbacks involving the influence of both N fixation and denitrification on oceanic fixed-N inventories have been proposed as well (Deutsch et al., 2004). Although pre-Quaternary $\delta^{15}\text{N}_{\text{sed}}$ variation has been reported, including highly ^{15}N -depleted (-4 to 0 ‰) Jurassic-Cretaceous units (Rau et al., 1987; Jenkyns et al., 2001; Junium and Arthur, 2007) and highly ^{15}N -enriched ($+6$ to $+14$ ‰) Carboniferous units (Algeo et al., 2008), the Phanerozoic record of marine N-isotopic variation and its relationship to long-term (i.e., multimillion-year) climate change have not been systemically investigated to date (Algeo and Meyers, 2009). Additional study of the marine N cycle is needed to better understand its relationship to organic carbon burial and long-term climate change and to more accurately parameterize N fluxes in general circulation models. In this study, we document variation in $\delta^{15}\text{N}_{\text{sed}}$ from 660 Ma to the present, demonstrating a strong relationship to first-order climate cycles, with lower $\delta^{15}\text{N}$ during greenhouse intervals and higher $\delta^{15}\text{N}$ during icehouse intervals. This pattern suggests that long-term variation in the marine N cycle is controlled by first-order tectonic cycles, and that it is linked to – and possibly a driver of – long-term climate change.

2 Methods

This study is based on the N-isotope distributions of 153 marine units ranging in age from the Neoproterozoic (660 Ma) to the early Quaternary (~ 2 Ma) (Fig. 1). Among these units are 35 that were analyzed specifically for this study (see isotopic methods, Appendix A), 33 that were taken from our own earlier research publications, and 85 that were taken from other published reports. For each study unit, we determined the median (50th percentile), standard deviation range (16th and 84th percentiles), and full range (minimum and maximum values) of its $\delta^{15}\text{N}$ distribution (Supplement Table 1). We also report organic $\delta^{13}\text{C}$ distributions as well as means for %TOC (total organic

BGD

10, 14769–14813, 2013

Icehouse-greenhouse variations in marine denitrification

T. J. Algeo et al.

Title Page

Abstract

Introduction

Conclusions

References

Tables

Figures

◀

▶

◀

▶

Back

Close

Full Screen / Esc

Printer-friendly Version

Interactive Discussion



carbon), %N, and molar $C_{\text{org}}:N$ ratios, where available (Supplement Table 1). The ages of all units were adjusted to the 2012 geologic timescale (Gradstein et al., 2012), as were the age ranges of the Phanerozoic icehouse and greenhouse climate modes in Fig. 1 (Montañez et al., 2011). A LOWESS curve was calculated for the entire dataset per the methods of Appendix B.

3 Results

Our $\delta^{15}N_{\text{sed}}$ dataset exhibits a mean of $+2.0 \pm 3.1$ ‰ with a range of -5.2 to $+10.4$ ‰ (Supplement Table 1; $n = 153$). $\delta^{15}N_{\text{sed}}$ values are mostly intermediate (0 to $+3$ ‰) during the late Cryogenian to early Ediacaran, low (-5 to 0 ‰) during the late Ediacaran to mid-Ordovician, intermediate during the late Ordovician to early Mississippian, high ($+3$ to $+10$ ‰) during the late Mississippian to Pennsylvanian, intermediate during the Triassic to early Cretaceous, low during the mid-Cretaceous, and intermediate to high during the late Cretaceous to Recent (Fig. 1). The modeled LOWESS curve for the Phanerozoic exhibits a minimum of -2.8 ‰ in the Cambrian and a maximum of $+8.0$ ‰ in the Mississippian; its variance ranges from 1.8 to 5.8 ‰ but is mostly 2–4 ‰. The most abrupt changes in $\delta^{15}N_{\text{sed}}$ are associated with a ~ 6 ‰ rise during the mid-Mississippian and a ~ 5 ‰ rise during the late Cretaceous. The $\delta^{15}N_{\text{sed}}$ dataset shows a strong relationship to first-order climate cycles, with low values during the greenhouse climate modes of the mid-Paleozoic and mid-Mesozoic and high values during the icehouse climate modes of the Late Paleozoic and Cenozoic (Fig. 1).

The $\delta^{15}N_{\text{sed}}$ dataset exhibits pronounced secular variation (i.e., a range of > 10 ‰) and strong secular coherence (i.e., 74% of total variance is accounted for by the LOWESS curve). The secular coherence of the dataset is significant in view of the relatively short residence time of nitrate in seawater (~ 3 kyr) (Tyrrell, 1999; Brandes and Devol, 2002), which theoretically offers potential for strong $\delta^{15}N_{\text{NO}_3^-}$ variation at intermediate (10^3 – 10^6 yr) timescales (Deutsch et al., 2004). Indeed, sub-Recent ma-

BGD

10, 14769–14813, 2013

Icehouse-greenhouse variations in marine denitrification

T. J. Algeo et al.

Title Page

Abstract

Introduction

Conclusions

References

Tables

Figures

◀

▶

◀

▶

Back

Close

Full Screen / Esc

Printer-friendly Version

Interactive Discussion



the bacterial use of nitrate as an oxidant in the respiration of organic matter with a maximum fractionation of $\sim -27\text{‰}$ (but commonly with an effective fractionation of $\sim -20 \pm 3\text{‰}$), resulting in a strongly ^{15}N -enriched residual seawater nitrate pool. Denitrification in suboxic marine sediments typically yields much lower net fractionation (~ -1 to -3‰) owing to near-quantitative utilization of porewater nitrate (Sigman et al., 2003; Lehmann et al., 2004). The anammox reaction, in which ammonium and nitrate (or nitrite) are converted to N_2 , may eliminate more fixed N than denitrification in some marine environments (Kuypers et al., 2005), although the isotopic fractionation associated with this process is not well known (Galbraith et al., 2008).

The N-isotopic composition of marine sediment depends on the $\delta^{15}\text{N}$ of seawater fixed N, fractionation during assimilatory uptake, and subsequent alteration during decay in the water column and sediment (Robinson et al., 2012). Both ammonium and nitrate can be used as N sources in primary production, with fractionations of $-10 \pm 5\text{‰}$ and $-3 \pm 2\text{‰}$, respectively (Hoch et al., 1994; Waser et al., 1998). Nitrate is by far the more important source of N for eukaryotic marine algae, but ammonium is utilized by some modern microbial communities (Hoch et al., 1994) and may have been the main N substrate for eukaryotic algae during some OAEs (Altabet, 2001; Higgins et al., 2012). Assimilatory uptake enriches the residual fixed N pool in ^{15}N and can result in shifts in the $\delta^{15}\text{N}_{\text{NO}_3^-}$ of local watermasses (Hoch et al., 1994), but quantitative utilization of fixed N by marine autotrophs at annual timescales normally limits fractionation due to this process (Sigman et al., 2000; Somes et al., 2010). These processes determine the N isotopic composition of primary marine organic matter, before modification by diagenesis.

4.2 Influence of diagenesis on sediment $\delta^{15}\text{N}$

Diagenesis has the potential to alter the N isotopic composition of organic matter through two main effects. First, selective degradation of proteins and amino acids, which are enriched in ^{15}N compared to more resistant compounds such as lipids and lignin, results in a shift toward lower $\delta^{15}\text{N}_{\text{sed}}$ (Prahl et al., 1997; Gaye-Haake et al.,

14774

BGD

10, 14769–14813, 2013

Icehouse-greenhouse variations in marine denitrification

T. J. Algeo et al.

Title Page

Abstract

Introduction

Conclusions

References

Tables

Figures

⏪

⏩

◀

▶

Back

Close

Full Screen / Esc

Printer-friendly Version

Interactive Discussion



Icehouse-greenhouse variations in marine denitrification

T. J. Algeo et al.

[Title Page](#)[Abstract](#)[Introduction](#)[Conclusions](#)[References](#)[Tables](#)[Figures](#)[◀](#)[▶](#)[◀](#)[▶](#)[Back](#)[Close](#)[Full Screen / Esc](#)[Printer-friendly Version](#)[Interactive Discussion](#)

2005). Second, aerobic bacterial decomposition of organic matter results in deamination, i.e., the release of isotopically light NH_4^+ (Macko and Estep, 1984; Macko et al., 1987; Holmes et al., 1999), which results in ^{15}N enrichment of the sinking flux of organic carbon by a few per mille (Altabet, 1988; Libes and Deuser, 1988; François et al., 1992; Saino, 1992; Lourey et al., 2003). Following burial, nitrification can enrich the porewater NH_4^+ pool in ^{15}N by 4–5%, potentially leading to changes in bulk-sediment $\delta^{15}\text{N}$ if NH_4^+ diffuses back to the water column (Brandes and Devol, 1997; Prokopenko et al., 2006). However, if NH_4^+ generated within the sediment is captured by clay minerals, then the bulk sediment may show little or no change in $\delta^{15}\text{N}$ relative to the organic sinking flux (Higgins et al., 2012). Because decay processes can have variable effects on $\delta^{15}\text{N}_{\text{sed}}$, net fractionation can be either positive or negative relative to the unaltered source material. Surface sediments tend to be enriched in ^{15}N by 1–5‰ relative to particulate organic nitrogen in the water column, possibly because the latter has undergone less extensive deamination (Brandes and Devol, 1997; Gaye-Haake et al., 2005; Prokopenko et al., 2006; Higgins et al., 2010). Differences between the $\delta^{15}\text{N}$ of the sinking and sediment fractions show water-depth dependence, reflecting greater oxic degradation of organic matter settling to the deep-ocean floor, although this effect is relatively small (Robinson et al., 2012). In contrast, rapid burial of organic matter in continental shelf and shelf-margin settings can yield sediment $\delta^{15}\text{N}$ values that are little modified from that of the organic export flux (Altabet and François, 1994; Altabet, 2001; Robinson et al., 2012).

Studies of N subfractions have been undertaken with the goal of recovering a N isotopic signature that is comparatively free of diagenetic effects. Chlorin N (Higgins et al., 2010) is ^{15}N -depleted relative to bulk-sediment N due to a ~5‰ fractionation during photosynthesis (Sachs et al., 1999). Some studies have claimed large (up to 5‰) shifts in bulk-sediment $\delta^{15}\text{N}$ as a consequence of diagenesis (Sachs and Repeta, 1999). However, the studies of N subfractions cited above exhibit a systematic offset of 3–5‰ between bulk-sediment and compound-specific $\delta^{15}\text{N}$ values that is consistent with the effects of photosynthetic fractionation overprinted by, at most, small (<2‰)

diagenetic effects. Following early diagenesis, deeper burial rarely causes more than minor changes in N-isotopic compositions, as shown by (1) $\delta^{15}\text{N}$ variation of only a few per mille over a wide range of metamorphic grades (Imbus et al., 1992; Busigny et al., 2003; Jia and Kerrich, 2004), and (2) $\delta^{15}\text{N}$ values for metamorphosed units that are virtually indistinguishable from those of coeval unmetamorphosed units (e.g., compare the Eocene-Jurassic Franciscan Complex with age-equivalent units; Supplement Table 1). Ancient marine sediments are thus considered to be fairly robust recorders of the ambient isotopic composition of seawater fixed N (Altabet and François, 1994; Altabet et al., 1995; Higgins et al., 2010; Robinson et al., 2012).

4.3 Influence of organic matter source on sediment $\delta^{15}\text{N}$

All of the data used in this study represent bulk-sediment N-isotopic compositions, thus including both organic and inorganic nitrogen. The amount of mineral N present in most marine sediments is so small that it typically has little influence on bulk-sediment $\delta^{15}\text{N}$ (Holloway et al., 1998; Holloway and Dahlgren, 1999). In contrast, clay-adsorbed N (principally ammonium) can be quantitatively important, with concentrations of ~0.1–0.2% in some marine units (e.g., Fig. 3 in Meyers, 1997; Fig. 3 in Lücke and Brauer, 2004; and Fig. S1 in Algeo et al., 2008). However, clay-adsorbed N is mostly derived from sedimentary organic matter, and the organic-to-clay transfer of nitrogen is often at a late diagenetic stage, thus limiting translocation of N within the sediment column (Macko et al., 1986). These considerations suggest that the presence of a small inorganic N fraction in the study units is unlikely to affect our results.

In compiling the $\delta^{15}\text{N}_{\text{sed}}$ dataset used in the present study, our principal concern was that admixture of large amounts of terrestrially sourced organic N might bias the marine $\delta^{15}\text{N}$ record. A number of different procedures can be used to screen samples for the presence of terrestrial organic matter, including petrographic analysis to identify maceral types (Hutton, 1987), biomarker analysis of steroids, polysaccharides, and hopane and tricyclic ratios (Huang and Meischein, 1979; Frimmel et al., 2004; Peters et al., 2004; Grice et al., 2005; Sephton et al., 2005; Wang and Visscher, 2007; Xie et

[Title Page](#)

[Abstract](#)

[Introduction](#)

[Conclusions](#)

[References](#)

[Tables](#)

[Figures](#)



[Back](#)

[Close](#)

[Full Screen / Esc](#)

[Printer-friendly Version](#)

[Interactive Discussion](#)



al., 2007; Algeo et al., 2012), and hydrogen and oxygen indices (HI-OI) (Espitalié et al., 1977, 1985; Peters, 1986). Such proxies are generally reliable in distinguishing organic matter sources with some caveats (Meyers et al., 2009a). These types of proxies were available only for a subset of the present study units (Supplement Table 1) but, where available, they generally confirmed the dominance of marine over terrestrial organic matter. Studies of modern continental shelf sediments show a rapid decline in the proportion of terrestrial organic matter away from coastlines (Hedges et al., 1997; Hartnett et al., 1998). The study units of Proterozoic to Jurassic age were mostly epicontinental and, hence, deposited close to land areas (Fig. 2), although there was little terrestrial vegetation for export to marine systems prior to the Devonian (Kenrick and Crane, 1997). In contrast, the study units of Cretaceous to Recent age (which are mostly from DSDP, ODP, and IODP cores) overwhelmingly represent open-ocean and distal continent-margin sites at a significant remove from land areas (Fig. 2) and, hence, that were unlikely to have accumulated large amounts of terrestrial organic matter.

Sediment $C_{org} : N$ ratios potentially also provide insights regarding organic matter sources (Meyers, 1994, 1997). Terrestrial organic matter is characterized by high $C_{org} : N$ ratios (~ 20 – 200) owing to an abundance of N-poor cellulose in land plants (Ertel and Hedges, 1985). In contrast, fresh marine organic matter exhibits low $C_{org} : N$ ratios (~ 4 – 10) owing to a lack of cellulose and an abundance of N-rich proteins in planktic algae (Müller, 1977). Diagenesis can result in either lower $C_{org} : N$ ratios through preferential preservation of organic N as clay-adsorbed ammonium, or higher $C_{org} : N$ ratios through preferential loss of proteinaceous components (Meyers, 1994). Covariation between $\delta^{15}N$, $\delta^{13}C_{org}$, and $C_{org} : N$ ratios can reveal mixing relationships in estuarine (Thornton and McManus, 1994; Ogrinc et al., 2005) and marine sediments (Müller, 1977; Meyers et al., 2009b). In our Phanerozoic dataset, $\delta^{13}C_{org}$ and $\delta^{15}N$ exhibit no relationship ($r^2 = 0.01$; Fig. 3), but $\delta^{15}N$ exhibits moderate negative covariation with $C_{org} : N$ ($r^2 = 0.21$; $p(\alpha) < 0.001$; Fig. 4). The source of the latter relationship is uncertain. Although conceivably representing a marine-terrestrial mixing trend, this interpretation is unlikely given that the majority of units with low $\delta^{15}N$ and high $C_{org} : N$ values

BGD

10, 14769–14813, 2013

Icehouse-greenhouse variations in marine denitrification

T. J. Algeo et al.

Title Page

Abstract

Introduction

Conclusions

References

Tables

Figures

◀

▶

◀

▶

Back

Close

Full Screen / Esc

Printer-friendly Version

Interactive Discussion



come from open-marine settings of Cretaceous-Recent age that presumably contain little terrestrial organic matter. The linkage of higher $C_{org} : N$ ratios (to ~ 40) with lower $\delta^{15}N$ values is particularly characteristic of organic-rich sediments deposited under anoxic conditions (e.g., Junium and Arthur, 2007). This pattern has been attributed to enhanced cyanobacterial N fixation under N-poor conditions in restricted anoxic marine basins (Junium and Arthur, 2007) but potentially might be due to enhanced assimilatory recycling of ^{15}N -depleted ammonium in such settings (Higgins et al., 2012).

The relatively N-poor nature of terrestrial organic matter means that, even if present in modest quantities, it is unlikely to have had much influence on bulk sediment $\delta^{15}N$. For example, in a 50 : 50 mixture of marine and terrestrial organic matter, ~ 80 – 95 % of total N will be of marine origin because of the lower $C_{org} : N$ ratios of marine organic matter (~ 4 – 10) relative to terrestrial organic matter (~ 20 – 200) (Meyers, 1994, 1997). Where mixing proportions have been quantified, the terrestrial organic fraction is more commonly in the range of 10–20 % (e.g., Jaminski et al., 1998; Algeo et al., 2008), in which case > 95 % of total N is marine-derived. Although we cannot conclusively demonstrate that our Phanerozoic marine $\delta^{15}N$ trend (Fig. 1) is uninfluenced by terrestrial contamination, we infer that such influences were probably minimal, and that the observed pattern of secular variation in $\delta^{15}N_{sed}$ broadly reflects the isotopic composition of contemporaneous seawater fixed N.

4.4 Influence of depositional setting on sediment $\delta^{15}N$

One important issue is whether our $\delta^{15}N_{sed}$ dataset records variation in a global parameter (i.e., seawater nitrate $\delta^{15}N$) or represents mainly local watermass effects in which sediment $\delta^{15}N$ varied as a function of depositional setting. Owing to unevenness in the distribution of depositional settings in our dataset through time, we cannot answer this question definitively, but the following analysis provides some insight as to the relative importance of local versus global controls on sediment $\delta^{15}N$.

BGD

10, 14769–14813, 2013

Icehouse-greenhouse variations in marine denitrification

T. J. Algeo et al.

Title Page

Abstract

Introduction

Conclusions

References

Tables

Figures

⏪

⏩

◀

▶

Back

Close

Full Screen / Esc

Printer-friendly Version

Interactive Discussion



Icehouse-greenhouse variations in marine denitrification

T. J. Algeo et al.

Title Page

Abstract

Introduction

Conclusions

References

Tables

Figures

◀

▶

◀

▶

Back

Close

Full Screen / Esc

Printer-friendly Version

Interactive Discussion



variation in the intensity of water-column denitrification, which was higher in the high-productivity oceanic cul-de-sac formed by the Tethys Ocean (Mii et al., 2001; Grossman et al., 2008) and in the northwest Pangean upwelling system (Beauchamp and Baud, 2002; Schoepfer et al., 2012, 2013). Despite major changes in seawater temperature and dissolved oxygen levels in conjunction with the PTB crisis (Romano et al., 2012; Sun et al., 2012; Song et al., 2013), marine units show remarkably little change in $\delta^{15}\text{N}$ across the PTB: Lower Triassic unit-means range from -0.4‰ to $+5.3\text{‰}$, and the magnitude of the PTB shift at individual locales varies from -2.8 to $+0.4\text{‰}$ with an average of -0.9‰ . Negative $\delta^{15}\text{N}_{\text{sed}}$ shifts at the PTB have been attributed to enhanced N fixation rates (Luo et al., 2011). However, these shifts are consistent with our hypothesis of lowered seawater $\delta^{15}\text{N}_{\text{NO}_3^-}$ values as a consequence of increased importance of sedimentary (relative to water-column) denitrification during greenhouse climate intervals such as that of the Early Triassic (Romano et al., 2012; Sun et al., 2012).

4.5 Marine nitrogen cycle modeling

We employed a reservoir box model to investigate possible controls on long-term secular variation in seawater $\delta^{15}\text{N}_{\text{NO}_3^-}$ (see Appendix C for model details). Seawater $\delta^{15}\text{N}_{\text{NO}_3^-}$ can be approximated from a steady-state isotope mass balance that assumes N fixation (f_{FIX}) as the primary source and sedimentary (f_{DS}) and water-column (f_{DW}) denitrification as the two largest sinks for seawater fixed N (Brandes and Devol, 2002; Deutsch et al., 2004; Gruber, 2008). We assumed that the marine N cycle is in a homeostatic steady state condition at geologic timescales (DeVries et al., 2013), and thus that losses of fixed N to denitrification are balanced by new N fixation (i.e., $f_{\text{DW}} + f_{\text{DS}} = f_{\text{FIX}}$), which is consistent with the strong spatial coupling of these processes in the modern ocean (Galbraith et al., 2004; Deutsch et al., 2007; Knapp et al., 2008). Our baseline scenario utilized fluxes and fractionation factors based on the modern marine N cycle, i.e., $f_{\text{FIX}} = 220 \text{ Tg a}^{-1}$, $f_{\text{DS}} = 160 \text{ Tg a}^{-1}$, $f_{\text{DW}} = 60 \text{ Tg a}^{-1}$, $\epsilon_{\text{FIX}} = -2\text{‰}$,

$\varepsilon_{DS} = -2\text{‰}$, and $\varepsilon_{DW} = -20\text{‰}$, where ε represents the fractionations associated with N source and sink fluxes (f), and the photosynthetic fractionation factor (ε_P) linked to nitrate utilization is 0‰ . This scenario yields an equilibrium seawater $\delta^{15}\text{N}_{\text{NO}_3^-}$ of $+4.9\text{‰}$ that matches the composition of fixed N in the present-day deep ocean (Sigman et al., 2000).

The most important influence on global seawater $\delta^{15}\text{N}_{\text{NO}_3^-}$ variation in our model is the fraction of denitrification that occurs in the water column (F_{DW} , calculated as $f_{DW} / (f_{DW} + f_{DS})$; Fig. 8). In our baseline scenario ($\varepsilon_{DW} = -20\text{‰}$, $\varepsilon_P = 0\text{‰}$), the modern seawater $\delta^{15}\text{N}_{\text{NO}_3^-}$ of $\sim +4.9\text{‰}$ corresponds to F_{DW} of 0.27 (point 1, Fig. 8b), which is close to recent estimates of 0.29 (DeVries et al., 2012) and 0.36 (Eugster and Gruber, 2012). However, the same $\delta^{15}\text{N}_{\text{NO}_3^-}$ composition can be achieved with other model parameterizations. Laboratory culture studies indicate that ε_{DW} might be as low as -10‰ in some marine systems (Kritee et al., 2012). Reducing ε_{DW} to -15‰ and -10‰ yields F_{DW} of 0.37 and 0.62 (points 2 and 3, Fig. 8b); the former is still within the range of F_{DW} estimates for modern marine systems (cf. Eugster and Gruber, 2012) although the latter is not. Our baseline scenario assumes no net fractionation linked to photosynthetic assimilation of seawater nitrate ($\varepsilon_P = 0\text{‰}$) (Brandes and Devol, 2002; Gruber, 2008; Granger et al., 2010). Uptake of ammonium is accompanied by a significant negative fractionation (Hoch et al., 1994; Waser et al., 1998), and a recent study proposed that recycled ammonium was a major source of fixed N for eukaryotic algae during some OAEs (Higgins et al., 2012). We modeled the effects of variable photosynthetic fractionation with ε_P values of -4 and -8‰ , which yield $\delta^{15}\text{N}_{\text{NO}_3^-}$ equal to $+4.9\text{‰}$ when F_{DW} is 0.48 and 0.72, respectively (points 4 and 5, Fig. 8b). These F_{DW} values are improbably large for the modern (icehouse) marine N cycle, but non-zero values of ε_P may have been important during greenhouse intervals (see below).

The variations in seawater $\delta^{15}\text{N}_{\text{NO}_3^-}$ between icehouse and greenhouse climate modes observed in our long-term $\delta^{15}\text{N}_{\text{sed}}$ record (Fig. 1) are an indication of major secular changes in the marine N cycle. In our baseline scenario, the peak ice-

Icehouse-greenhouse variations in marine denitrification

T. J. Algeo et al.

[Title Page](#)[Abstract](#)[Introduction](#)[Conclusions](#)[References](#)[Tables](#)[Figures](#)[◀](#)[▶](#)[◀](#)[▶](#)[Back](#)[Close](#)[Full Screen / Esc](#)[Printer-friendly Version](#)[Interactive Discussion](#)

Icehouse-greenhouse variations in marine denitrification

T. J. Algeo et al.

Title Page

Abstract

Introduction

Conclusions

References

Tables

Figures

◀

▶

◀

▶

Back

Close

Full Screen / Esc

Printer-friendly Version

Interactive Discussion



house $\delta^{15}\text{N}_{\text{NO}_3^-}$ of $\sim +8\text{‰}$ yields F_{DW} of ~ 0.45 (point 6, Fig. 8b), indicating an increase in water-column denitrification relative to the modern ocean. Although the same $\delta^{15}\text{N}_{\text{NO}_3^-}$ can be achieved with ε_{DW} of -15‰ and -10‰ , the resulting F_{DW} values (0.62 and 0.98; points 7 and 8, Fig. 8b) are improbably large. Lack of evidence for ammonium recycling during icehouse modes makes non-zero ε_{P} values unlikely, which in any case would yield equally improbable values of F_{DW} . The minimum greenhouse $\delta^{15}\text{N}_{\text{NO}_3^-}$ of $\sim -3\text{‰}$ cannot be achieved in our baseline scenario even when F_{DW} is reduced to 0 (point 9, Fig. 8b). However, evidence for strong ammonium recycling in greenhouse oceans (Higgins et al., 2012) indicates that ε_{P} may have been non-zero at those times. Decreasing ε_{P} to -4 and -8‰ yields F_{DW} of 0.10 and 0.33 (points 10 and 11, Fig. 8b), the former representing a large decrease in F_{DW} relative to the modern ocean. Since ε_{P} of -8‰ represents an absolute minimum (i.e., recycling of nearly all seawater N as ammonium), $\varepsilon_{\text{P}} = -4\text{‰}$ is a more reasonable estimate for anoxic marine systems with mixed utilization of recycled ammonium and cyanobacterially fixed N (Higgins et al., 2012). Also, strong ammonium recycling in greenhouse oceans requires near-quantitative removal of nitrate via water column denitrification ($F_{\text{DW}} = 1$) in order to maintain a near-surface ammonium pool (Higgins et al., 2012). In this case, the apparent isotope effect associated with water column denitrification approaches 0%, analogous to sedimentary denitrification and the control on the isotopic composition of sinking organic matter is set by fractionation associated with ammonium assimilation. Note that, at low F_{DW} , variation in ε_{DW} has little effect on $\delta^{15}\text{N}_{\text{NO}_3^-}$. In summary, the most likely scenario to account for long-term secular shifts in $\delta^{15}\text{N}_{\text{NO}_3^-}$ (Fig. 1) within existing N-budget and isotopic constraints is for (1) F_{DW} to vary between ~ 0.2 and 0.5 (permissive of ε_{DW} values between -15 and -20‰) with $\varepsilon_{\text{P}} = 0\text{‰}$ during icehouse climate modes, and (2) F_{DW} to decrease to ~ 0.1 – 0.2 with a shift in ε_{P} to ca. -4‰ during greenhouse climate modes.

4.6 Controls on long-term variation in the marine nitrogen cycle

Although enhanced water-column denitrification has been inferred during the warm climate intervals that produced oceanic anoxic events (OAEs) (Rau et al., 1987; Jenkyns et al., 2001; Junium and Arthur, 2007), strong ^{15}N -depletion of contemporaneous sediments is inconsistent with globally elevated water-column denitrification rates. Our inference of reduced water-column denitrification during greenhouse climate modes (Fig. 9a) contradicts the existing paradigm linking OAEs to high water-column denitrification rates (Rau et al., 1987; Jenkyns et al., 2001; Junium and Arthur, 2007). A reconciliation of these views is possible if rates were high regionally in semi-restricted marine basins such as the proto-South Atlantic but reduced on a globally integrated basis. Our results are also at odds with the observation that modern upwelling zones exhibit peak $\delta^{15}\text{N}_{\text{sed}}$ values in conjunction with deglaciations rather than glacial maxima (François et al., 1992; Altabet et al., 1995; Ganeshram et al., 1995). While the latter relationship is valid at intermediate timescales, our results indicate that F_{DW} is higher *on a time-averaged basis* (i.e., integrating glacial-interglacial variation) for icehouse modes than for greenhouse modes. This inference is supported by a study of Plio-Pleistocene sediments in the eastern tropical Pacific, in which $\delta^{15}\text{N}_{\text{sed}}$ rose by $\sim 2\text{‰}$ following a cooling event at 2.1 Ma (Liu et al., 2008), consistent with an increase in time-averaged water-column denitrification rates. We infer that transient, albeit repeated shifts in favor of water-column denitrification (i.e., higher F_{DW}) during the interglacial stages of icehouse climate intervals have resulted in a sustained (i.e., multimillion-year) shift toward higher seawater $\delta^{15}\text{N}_{\text{NO}_3^-}$ that has been captured by the long-term $\delta^{15}\text{N}_{\text{sed}}$ record (Fig. 1).

Several mechanisms might potentially link variations in seawater $\delta^{15}\text{N}_{\text{NO}_3^-}$ to long-term climate cycles. Eustatic variation is known to influence the locus of denitrification in marine systems (Deutsch et al., 2004). High eustatic elevations during greenhouse climate modes favor sedimentary denitrification owing to greater burial of organic matter on continental shelves (Fig. 9a), and low eustatic elevations during icehouse cli-

BGD

10, 14769–14813, 2013

Icehouse-greenhouse variations in marine denitrification

T. J. Algeo et al.

Title Page

Abstract

Introduction

Conclusions

References

Tables

Figures

◀

▶

◀

▶

Back

Close

Full Screen / Esc

Printer-friendly Version

Interactive Discussion



mate modes favor water-column denitrification through elevated organic carbon sinking fluxes to the thermocline and expansion of oceanic oxygen-minimum zones (Fig. 9b). A first-order eustatic control on the marine N cycle is consistent with existing Phanerozoic eustatic reconstructions (Haq and Schutter, 2008), which show major sea-level falls in the Visean (early Mississippian) and Campanian (late Cretaceous) linked to growth of continental icesheets and a transition from greenhouse to icehouse conditions (Fig. 1). Alternatively, long-term variation in the marine N cycle may reflect tectonic controls, e.g., changes in oceanic gateways and circulation patterns that altered the locus of denitrification through changes in upwelling intensity or thermocline ventilation. For example, the early Mississippian was a time of closure of an equatorial seaway in the Rheic Ocean region (Saltzman, 2003), and the late Cretaceous coincided with widening of the central and south Atlantic basins and a shift of deepwater formation into the North Atlantic region (MacLeod and Huber, 1996). Although further investigation will be needed, these examples show that the marine N cycle is intimately linked to first-order tectonic cycles and, possibly, may have a major influence on long-term climate change.

5 Conclusions

The present analysis of $\delta^{15}\text{N}$ variation in 153 marine sedimentary units ranging in age from the Neoproterozoic to the Quaternary is the first to assess long-term variation in the marine N cycle and controls thereon. Variation in $\delta^{15}\text{N}_{\text{sed}}$, which serves as a proxy for seawater nitrate $\delta^{15}\text{N}$, exhibits strong secular coherence since 660 Ma, with 74 % of total variance accounted for by a LOWESS trend. This pattern is surprising because the short residence time of fixed N in modern seawater (≤ 3 kyr) suggests that short-term variation in the marine N cycle has the potential to dominate the sedimentary N-isotope record and produce no coherent long-term patterns. Average $\delta^{15}\text{N}_{\text{sed}}$ ranges from lower values (~ -2 to $+2$ ‰) during greenhouse climate modes of the mid-Paleozoic and mid-Mesozoic to higher $\delta^{15}\text{N}$ ($\sim +4$ to $+8$ ‰) during icehouse climate modes of the Late Paleozoic and Cenozoic. This pattern suggests that long-term varia-

Icehouse-greenhouse variations in marine denitrification

T. J. Algeo et al.

Title Page

Abstract

Introduction

Conclusions

References

Tables

Figures



Back

Close

Full Screen / Esc

Printer-friendly Version

Interactive Discussion



tion in the marine N cycle is controlled by first-order tectonic cycles, and that it is linked to – and possibly a driver of – long-term climate change. We tentatively link long-term variation in the marine nitrogen cycle to global sea-level changes and shifts in the dominant locus of denitrification, with sedimentary denitrification and water-column denitrification dominant during greenhouse highstands and icehouse lowstands, respectively, a relationship confirmed by reservoir box modeling. These results also challenge the widely held idea that oceanic anoxic events (OAEs) were associated with elevated rates of water-column denitrification. Rather, the present study shows that globally integrated water-column denitrification rates must have been lower during greenhouse intervals (when OAEs developed) relative to icehouse intervals.

Appendix A

Stable isotopic analyses

For most analyses original to this study, C and N elemental and stable isotopic compositions were determined at the University of Texas at Arlington Stable Isotope Laboratory using a Costech 5010 elemental analyzer coupled via a ConFlo-III device to a ThermoFinnigan Delta*Plus*XP isotope-ratio-mass spectrometer. Analytical precision was 0.08 ‰ for %N, 0.07 ‰ for %C, 0.05 ‰ for $\delta^{15}\text{N}$, and 0.09 ‰ for $\delta^{13}\text{C}$ of the laboratory standards. All isotopic results are reported relative to air ($\delta^{15}\text{N}$) and V-PDB ($\delta^{13}\text{C}$). A subset of samples used in this study was analyzed in the stable isotope laboratory at the University of Arizona and the University of Nevada at Las Vegas.

BGD

10, 14769–14813, 2013

Icehouse-greenhouse variations in marine denitrification

T. J. Algeo et al.

Title Page

Abstract

Introduction

Conclusions

References

Tables

Figures

◀

▶

◀

▶

Back

Close

Full Screen / Esc

Printer-friendly Version

Interactive Discussion



Appendix B

Calculation of LOWESS trend

Long-term secular variation in our $\delta^{15}\text{N}_{\text{sed}}$ dataset was modeled using a LOWESS (LOcally WEighted Scatterplot Smoothing) procedure, which determines a best-fit trend for irregularly distributed time-series data using an inverse-distance-squared weight function (Cleveland et al., 1992). The LOWESS curve of Fig. 1 was calculated as:

$$\delta^{15}\text{N}_t = \Sigma \left(1 / \left(1 + ((t - t_i) / \lambda)^2 \right) \times \delta^{15}\text{N}_i \right) / \Sigma \left(1 / \left(1 + ((t - t_i) / \lambda)^2 \right) \right) \quad (\text{B1})$$

where $\delta^{15}\text{N}_t$ is the estimated mean $\delta^{15}\text{N}$ at a given time t , $\delta^{15}\text{N}_i$ and t_i are the N-isotopic composition and age of study unit i , and the summation was performed for $i = 1$ to 153 (i.e., the full $\delta^{15}\text{N}_{\text{sed}}$ dataset). The parameter λ determines the temporal range (or window) of the inverse-distance-squared weight function. Larger values of λ are appropriate for intervals of lower data density and will produce a smoother LOWESS curve. We varied λ from 10 Myr at 660 Ma to 2 Myr at 0 Ma to match temporal variation in data density. The standard deviation range for $\delta^{15}\text{N}$ at a given time t was calculated as the mean plus or minus the standard deviation (σ), with the latter determined as:

$$\sigma \left(\delta^{15}\text{N}_t \right) = \left(\Sigma \left(\left(\delta^{15}\text{N}_t - \delta^{15}\text{N}_i \right)^2 \times \left(1 / \left(1 + ((t - t_i) / \lambda)^2 \right) \right) \times \xi \right) / \Sigma \left(1 / \left(1 + ((t - t_i) / \lambda)^2 \right) \right) \right)^{0.5} \quad (\text{B2})$$

where ξ is the fractional standard deviation range of interest (i.e., 0.68 for $\pm 1\sigma$, 0.95 for $\pm 2\sigma$). This range is shown as the shaded field bracketing the LOWESS curve in Fig. 1.

BGD

10, 14769–14813, 2013

Icehouse-greenhouse variations in marine denitrification

T. J. Algeo et al.

Title Page

Abstract

Introduction

Conclusions

References

Tables

Figures

◀

▶

◀

▶

Back

Close

Full Screen / Esc

Printer-friendly Version

Interactive Discussion



Appendix C

Marine nitrogen cycle modeling

The N-isotopic composition of seawater nitrate ($\delta^{15}\text{N}_{\text{NO}_3^-}$) can be approximated from a steady-state isotope mass balance that assumes N fixation (f_{FIX}) as the primary source and sedimentary (f_{DS}) and water-column (f_{DW}) denitrification as the two largest sinks for seawater fixed N (Brandes and Devol, 2002; Deutsch et al., 2004; Gruber, 2008). We developed two reservoir box models of the marine N cycle: (1) a fully integrated version that incorporates all significant N reservoirs and fluxes in the Earth's exogenic system (Fig. C1a), and (2) a simplified version that includes only the most important source (i.e., cyanobacterial N fixation) and sink fluxes (sedimentary and water-column denitrification) for seawater nitrate (Fig. C1b). The two models yield similar results for $\delta^{15}\text{N}_{\text{NO}_3^-}$ under a wide range of conditions (see below), indicating that the simplified model provides a reasonably robust representation of the major influences on the N-isotopic composition of seawater nitrate. Because the fully integrated model will be developed further in a later study, our focus here is on the results of the simplified model.

In both models, all fluxes are first-order functions of source reservoir mass:

$$f_i = k_i \times M_{x(t)} \quad (\text{C1})$$

where f_i is the flux of interest, k_i its flux constant (Supplement Table 2), and M_x the mass of source reservoir x at a given time t . Temporal changes in reservoir mass from t to $t + 1$ were calculated as:

$$M_{a(t+1)} = M_{a,t} + \int_t^{t+1} (f_{\text{VOL}} + f_{\text{DT}} + f_{\text{DW}} + f_{\text{DS}} + f_{\text{ANX}} + f_{\text{W}} - f_{\text{FIX-T}} - f_{\text{DEP}} - f_{\text{FIX}}) \quad (\text{C2})$$

Icehouse-greenhouse variations in marine denitrification

T. J. Algeo et al.

Title Page

Abstract

Introduction

Conclusions

References

Tables

Figures

◀

▶

◀

▶

Back

Close

Full Screen / Esc

Printer-friendly Version

Interactive Discussion



$$M_{t(t+1)} = M_{t(t)} + \int_t^{t+1} (f_{\text{FIX-T}} - f_{\text{VOL}} - f_{\text{DT}} - f_{\text{RIV}}) \quad (\text{C3})$$

$$M_{o(t+1)} = M_{o(t)} + \int_t^{t+1} (f_{\text{RIV}} + f_{\text{DEP}} + f_{\text{FIX}} - f_{\text{DW}} - f_{\text{DS}} - f_{\text{ANX}} - f_{\text{BUR}}) \quad (\text{C4})$$

$$M_{s(t+1)} = M_{s(t)} + \int_t^{t+1} (t + 1)(f_{\text{BUR}} - f_{\text{W}}) \quad (\text{C5})$$

Equations (C2–C5) integrate source and sink fluxes over a specified time range t to $t + 1$ for the following processes: terrestrial nitrogen fixation (FIX-T), volatilization of soil nitrogen (VOL), terrestrial soil denitrification (DT), riverine flux of fixed N (RIV), oceanic nitrogen fixation (FIX), deposition of atmospheric nitrogen in ocean (DEP), water-column denitrification (DW), sedimentary denitrification (DS), anammox loss of fixed N (ANX), burial of organic nitrogen (BUR), and weathering (W) (Fig. C1a). The simplified version of the model is limited to the fluxes FIX, DW, and DS (Fig. C1b). Changes in the N-isotopic composition of a given reservoir $x(\delta_x)$ from t to $t + 1$ were calculated as:

$$\delta_{x(t+1)} = M_{x(t)} \times \delta_{x(t)} + \left(\sum_{i=1}^{10} \left(\int_t^{t+1} f_i \times (\delta_x + \varepsilon_i) \right) \right) / \left(M_{x(t)} + \sum_{i=1}^{10} \left(\int_t^{t+1} f_i \right) \right) \quad (\text{C6})$$

where ε_i is the fractionation associated with flux i . The equation above is an expression of isotopic mass balance, where the summation ($\sum i = 1$ to 10) for each reservoir x was limited to those fluxes (f_i) appearing in Eqs. (C2–C5).

Icehouse-greenhouse variations in marine denitrification

T. J. Algeo et al.

Title Page

Abstract

Introduction

Conclusions

References

Tables

Figures

◀

▶

◀

▶

Back

Close

Full Screen / Esc

Printer-friendly Version

Interactive Discussion



Icehouse-greenhouse variations in marine denitrification

T. J. Algeo et al.

Title Page

Abstract

Introduction

Conclusions

References

Tables

Figures

◀

▶

◀

▶

Back

Close

Full Screen / Esc

Printer-friendly Version

Interactive Discussion



We parameterized the model based on the modern marine N budget. The total mass of seawater nitrate is $\sim 8.0 \times 10^5$ Tg N (Brandes and Devol, 2002). Whether the present-day marine N cycle is in balance is a matter of debate (Codispoti, 1995; Brandes and Devol, 2002). Recent studies have documented strong spatial coupling of cyanobacterial N fixation and water-column denitrification in the modern ocean (Galbraith et al., 2004; Deutsch et al., 2007; Knapp et al., 2008), implying that short-term losses of fixed N are locally compensated. At longer timescales, losses of fixed N to denitrification must be balanced by new N fixation in order to maintain a N:P ratio in global seawater close to that of marine phytoplankton (16 : 1) (Tyrrell, 1999). Estimates of the fluxes associated with cyanobacterial N fixation (f_{FIX}), sedimentary denitrification (f_{DS}), and water-column denitrification (f_{DW}) vary widely in older literature, although recent analyses of large datasets are beginning to converge on a consensus range of values (DeVries et al., 2012, 2013; Eugster and Gruber, 2012; Großkopf et al., 2012). Estimates of f_{FIX} include 120–140 Tg a⁻¹ (Gruber and Sarmiento, 1997; Galloway et al., 2004; Gruber and Galloway, 2008), 131–134 Tg a⁻¹ (Eugster and Gruber, 2012), and 177 ± 8 Tg a⁻¹ (Großkopf et al., 2012). Total oceanic denitrification has been estimated at 145–185 Tg a⁻¹ (Gruber and Sarmiento, 1997; Galloway et al., 2004), 120–240 Tg a⁻¹ (DeVries et al., 2013), 230 ± 60 Tg a⁻¹ (DeVries et al., 2012), 230–285 Tg a⁻¹ (Middelburg et al., 1996), 240 Tg a⁻¹ (Gruber and Galloway, 2008), and > 400 Tg a⁻¹ (Codispoti, 2007). The relative importance of sedimentary versus water-column denitrification was not well-known in the past (Gruber and Sarmiento, 1997), but recent marine N budgets have provided independent estimates of each flux. Estimates for f_{DW} include 52 ± 13 Tg a⁻¹ (Eugster and Gruber, 2012) and 66 ± 6 Tg a⁻¹ (DeVries et al., 2012), while estimates for f_{DS} range from 93 ± 25 Tg a⁻¹ (Eugster and Gruber, 2012) to 164 ± 60 Tg a⁻¹ (DeVries et al., 2012) and > 300 Tg a⁻¹ (Codispoti, 2007).

The $\delta^{15}\text{N}$ of seawater nitrate in the deep ocean (i.e., the largest reservoir of fixed N) is +4.8 to +5.0 ‰ (Sigman et al., 2000). The $\delta^{15}\text{N}$ of present-day atmospheric N₂ is 0 ‰ (Mariotti, 1984), a value inferred to have been nearly invariant through time

Icehouse-greenhouse variations in marine denitrification

T. J. Algeo et al.

[Title Page](#)[Abstract](#)[Introduction](#)[Conclusions](#)[References](#)[Tables](#)[Figures](#)[⏪](#)[⏩](#)[◀](#)[▶](#)[Back](#)[Close](#)[Full Screen / Esc](#)[Printer-friendly Version](#)[Interactive Discussion](#)

(Berner, 2006). The fractionation associated with cyanobacterial N fixation of atmospheric N_2 (ϵ_{FIX}) is estimated to be -1 to -3 ‰ (Macko et al., 1987; Carpenter et al., 1997). Fractionation during water-column denitrification (ϵ_{DW}) has a maximum value of $\sim -27(\pm 3)$ ‰ (Gruber and Sarmiento, 1997; Barford et al., 1999; Voss et al., 2001; Murray et al., 2005), although the effective fractionation may be closer to -20 ‰ (Brandes and Devol, 2002). Recent culture studies have suggested that this fractionation might even be as low as -10 to -15 ‰ (Kritee et al., 2012), an idea that we explore in our modeling simulations. We did not parameterize the anammox reaction (Sigman et al., 2003) separately owing to significant uncertainties concerning the scale of this process and any associated fractionation. While this reaction is a major sink for seawater fixed N, possibly larger than water-column denitrification in some oceanic regions (Mulder et al., 1995; Kuypers et al., 2005), it is thought that field-based estimates of fractionation due to water-column denitrification have incorporated any effects related to anammox Thamdrup et al. (2006). Denitrification in suboxic marine sediments (ϵ_{DS}) typically yields a small net fractionation (~ -1 to -3 ‰) owing to near-quantitative utilization of porewater nitrate (Lehmann et al., 2004; Galbraith et al., 2008). However, this fractionation can range from ~ 0 ‰ in organic-rich, reactive sediments to as high as -5 to -7 ‰ in organic-lean, unreactive sediments (Lehmann et al., 2007). An estimate of -0.8 ‰ for the global mean fractionation due to sedimentary denitrification (Kuypers et al., 2005) does not take into account effects associated with the upward diffusive flux of ^{15}N -enriched ammonium in reactive sediments (Higgins et al., 2012). The fractionation associated with assimilation of seawater fixed N by eukaryotic marine algal (ϵ_P) can be as large as -5 to -8 ‰ for nitrate (Lehmann et al., 2007) but is more typically -1 to -3 ‰ (Macko et al., 1987; Carpenter et al., 1997). We assumed a net fractionation of 0 ‰ based on complete photosynthetic utilization of seawater nitrate at longer timescales. The fractionation associated with ammonium uptake by marine algae is $-10(\pm 5)$ ‰ (Brandes and Devol, 2002), and this process is more likely to yield a net fractionation owing to incomplete utilization of recycled ammonium in anoxic marine systems (Higgins et al., 2012).

The fully integrated and simplified marine N-cycle models exhibit similar results for seawater $\delta^{15}\text{N}_{\text{NO}_3^-}$ under a wide range of conditions. The models were tuned to yield identical F_{DW} of 0.27 for the baseline scenario, in which seawater $\delta^{15}\text{N}_{\text{NO}_3^-}$ is equal to +4.9‰ (Fig. C2). Varying F_{DW} from 0 to 0.5 yields a slightly smaller range of $\delta^{15}\text{N}_{\text{NO}_3^-}$ values for the fully integrated model (from +0.53 to +8.60‰) than for the simplified model (from +0 to +9.0‰), indicating that inclusion of secondary fluxes in the fully integrated model has a modest stabilizing effect on the isotopic composition of seawater nitrate. Differences in $\delta^{15}\text{N}_{\text{NO}_3^-}$ between the two models are < 0.4 ‰ for the range of F_{DW} (~ 0.1 – 0.5) that is most likely to characterize natural systems (Fig. C2). This outcome reflects the fact that the secondary fluxes present in the fully integrated model (e.g., atmospheric deposition, riverine transport, and burial; Fig. C1a) are generally either small in magnitude or associated with limited fractionations. Thus, the simplified model (Fig. C1b) provides a reasonably robust representation of the major influences on the N-isotopic composition of seawater nitrate.

Supplementary material related to this article is available online at <http://www.biogeosciences-discuss.net/10/14769/2013/bgd-10-14769-2013-supplement.pdf>.

Acknowledgements. We thank Craig Johnson, Leo Krystyn, Steven Lev, Jeff Over, Thomas Pedersen, Brad Sageman, Peter Sauer, and Shane Schoepfer for providing nitrogen isotopic data or sample material.

T. J. Algeo, P. A. Meyers, and R. S. Robinson developed the project, and all authors generated data, participated in data analysis, and drafted the manuscript.

BGD

10, 14769–14813, 2013

Icehouse-greenhouse variations in marine denitrification

T. J. Algeo et al.

Title Page

Abstract

Introduction

Conclusions

References

Tables

Figures

◀

▶

◀

▶

Back

Close

Full Screen / Esc

Printer-friendly Version

Interactive Discussion



References

- Algeo, T. J. and Meyers, P. A.: Icehouse-greenhouse climate impacts on the Phanerozoic marine nitrogen cycle, *Geol. Soc. Am. Abstr. Progr.*, 44, p. 458, 2009.
- Algeo, T. J., Rowe, H., Hower, J. C., Schwark, L., Hermann, A., and Heckel, P. H.: Oceanic denitrification during Late Carboniferous glacial-interglacial cycles, *Nat. Geosci.*, 1, 709–714, 2008.
- Algeo, T. J., Henderson, C. M., Ellwood, B., Rowe, H., Elswick, E., Bates, S., Lyons, T., Hower, J. C., Smith, C., Maynard, J. B., Hays, L. E., Summons, R. E., Fulton, J., and Freeman, K. H.: Evidence for a diachronous Late Permian marine crisis from the Canadian Arctic region, *Geol. Soc. Am. Bull.*, 124, 1424–1448, 2012.
- Altabet, M. A.: Variations in nitrogen isotopic composition between sinking and suspended particles: Implications for nitrogen cycling and particle transformation in the open ocean, *Deep-Sea Res. I*, 35, 535–554, 1988.
- Altabet, M. A.: Nitrogen isotopic evidence for micronutrient control of fractional NO_3^- utilization in the equatorial Pacific, *Limnol. Oceanogr.*, 46, 368–380, 2001.
- Altabet, M. A. and François, R.: Sedimentary nitrogen isotopic ratio as a recorder for surface ocean nitrate utilization, *Glob. Biogeochem. Cycles*, 8, 103–116, 1994.
- Altabet, M. A., François, R., Murray, D. W., and Prell, W. L.: Climate-related variations in denitrification in the Arabian Sea from sediment $^{15}\text{N}/^{14}\text{N}$ ratios, *Nature*, 373, 506–509, 1995.
- Barford, C. C., Montoya, J. P., Altabet, M. A., and Mitchell, R.: Steady-state nitrogen isotope effects of N_2 and N_2O production in *Paracoccus denitrificans*, *Appl. Env. Microbiol.*, 65, 989–994, 1999.
- Beauchamp, B. and Baud, A.: Growth and demise of Permian biogenic chert along north-west Pangea: evidence for end-Permian collapse of thermohaline circulation, *Palaeogeogr. Palaeoclimatol. Palaeoecol.*, 184, 37–63, 2002.
- Berner, R. A.: Geological nitrogen cycle and atmospheric N_2 over Phanerozoic time, *Geology*, 34, 413–415, 2006.
- Brandes, J. A. and Devol, A. H.: Isotopic fractionation of oxygen and nitrogen in coastal marine sediments, *Geochim. Cosmochim. Acta*, 61, 1793–1801, 1997.
- Brandes, J. A. and Devol, A. H.: A global marine-fixed nitrogen isotopic budget: implications for Holocene nitrogen cycling, *Glob. Biogeochem. Cy.*, 16, 1–14, 2002.

Icehouse-greenhouse variations in marine denitrification

T. J. Algeo et al.

Title Page

Abstract

Introduction

Conclusions

References

Tables

Figures

◀

▶

◀

▶

Back

Close

Full Screen / Esc

Printer-friendly Version

Interactive Discussion



Icehouse-greenhouse variations in marine denitrification

T. J. Algeo et al.

Title Page

Abstract

Introduction

Conclusions

References

Tables

Figures

◀

▶

◀

▶

Back

Close

Full Screen / Esc

Printer-friendly Version

Interactive Discussion



- Eugster, O. and Gruber, N.: A probabilistic estimate of global marine N-fixation and denitrification, *Glob. Biogeochem. Cy.*, 26, GC4013, doi:10.1029/2012GB004300, 2012.
- François, R., Altabet, M. A., and Burckle, L. H.: Glacial to interglacial changes in surface nitrate utilization in the Indian section of the Southern Ocean as recorded by sediment $\delta^{15}\text{N}$, *Paleoceanography*, 7, 589–606, 1992.
- Frimmel, A., Oschmann, W., and Schwark, L.: Chemostratigraphy of the Posidonia Black Shale, SW-Germany: I – Influence of sea level variation on organic facies evolution, *Chem. Geol.*, 206, 199–230, 2004.
- Galbraith, E. D., Kienast, M., Pedersen, T. F., and Calvert, S. E.: Glacial-interglacial modulation of the marine nitrogen cycle by high-latitude O_2 supply to the global thermocline, *Paleoceanography*, 19, 1–12, 2004.
- Galbraith, E. D., Sigman, D. M., Robinson, R. S., and Pedersen, T. F.: Nitrogen in past marine environments, in: *Nitrogen in the Marine Environment*, edited by: Capone, D. G., Bronk, D. A., Mulholland, M. R., and Carpenter, E. J., 2nd Edn., Elsevier, Amsterdam, 1497–1535, 2008.
- Galloway, J. N., Dentener, F. J., Capone, D. G., Boyer, E. W., Howarth, R. W., Seitzinger, S. P., Asner, G. P., Cleveland, C. C., Green, P. A., Holland, E. A., Karl, D. M., Michaels, A. F., Porter, J. H., Townsend, A. R., and Vörösmarty, C. J.: Nitrogen cycles: past, present, and future, *Biogeochemistry*, 70, 153–226, 2004.
- Ganeshram, R. S., Pedersen, T. F., Calvert, S. E., and Murray, J. W.: Large changes in oceanic nutrient inventories from glacial to interglacial periods, *Nature*, 376, 755–758, 1995.
- Gaye-Haake, B., Lahajnar, N., Emeis, K.-C., Unger, D., Rixen, T., Suthhof, A., Ramaswamy, V., Schulz, H., Paropkari, A. L., Guptha, M. V. S., and Ittekkot, V.: Stable nitrogen isotopic ratios of sinking particles and sediments from the northern Indian Ocean, *Mar. Chem.*, 96, 243–255, 2005.
- Gradstein, F. M., Ogg, J. G., Schmitz, M. D., and Ogg, G. M. (Eds.): *The Geologic Time Scale 2012*, 2 vols., Elsevier, Amsterdam, 1144 pp., 2012.
- Granger, J., Sigman, D. M., Rohde, M. M., Maldonado, M. T., and Tortell, P. D.: N and O isotope effects during nitrate assimilation by unicellular prokaryotic and eukaryotic plankton cultures, *Geochim. Cosmochim. Acta*, 74, 1030–1040, 2010.
- Grice, K., Cao, C., Love, G. D., Böttcher, M. E., Twitchett, R. J., Grosjean, E., Summons, R. E., Turgeon, S. C., Dunning, W., and Jin, Y.: Photic zone euxinia during the Permian-Triassic superanoxic event, *Science*, 307, 706–709, 2005.

Icehouse-greenhouse variations in marine denitrification

T. J. Algeo et al.

[Title Page](#)[Abstract](#)[Introduction](#)[Conclusions](#)[References](#)[Tables](#)[Figures](#)[◀](#)[▶](#)[◀](#)[▶](#)[Back](#)[Close](#)[Full Screen / Esc](#)[Printer-friendly Version](#)[Interactive Discussion](#)

Großkopf, T., Mohr, W., Baustian, T., Schunck, H., Gill, D., Kuypers, M. M. M., Lavik, G., Schmitz, R. A., Wallace, D. W. R., and LaRoche, J.: Doubling of marine dinitrogen-fixation rates based on direct measurements, *Nature*, 488, 361–364, 2012.

Grossman, E. L., Yancey, T. E., Jones, T. E., Bruckschen, P., Chuvashov, B., Mazzullo, S. J., and Mii, H. S.: Glaciation, aridification, and carbon sequestration in the Permo-Carboniferous: the isotopic record from low latitudes, *Palaeogeogr. Palaeoclimatol. Palaeoecol.*, 268, 222–233, 2008.

Gruber, N. G.: The marine nitrogen cycle: overview and challenges, in: *Nitrogen in the Marine Environment*, edited by: Capone, D. G., Bronk, D. A., Mulholland, M. R., and Carpenter, E. J., 2nd Edn., Elsevier, Amsterdam, 1–50, 2008.

Gruber, N. G. and Galloway, J. N.: An Earth-system perspective of the global nitrogen cycle, *Nature*, 451, 293–296, 2008.

Gruber, N. and Sarmiento, J.: Global patterns of marine nitrogen fixation and denitrification, *Glob. Biogeochem. Cy.*, 11, 235–266, 1997.

Haq, B. U. and Schutter, S. R.: A chronology of Paleozoic sea-level changes, *Science*, 322, 64–68, 2008.

Hartnett, H. E., Keil, R. G., Hedges, J. I., and Devol, A. H.: Influence of oxygen exposure time on organic carbon preservation in continental margin sediments, *Nature*, 391, 572–574, 1998.

Haug, G. H., Pedersen, T. F., Sigman, D. M., Calvert, S. E., Nielsen, B., and Peterson, L. C.: Glacial/interglacial variations in production and nitrogen fixation in the Cariaco Basin during the last 580 kyr, *Paleoceanography*, 13, 427–432, 1998.

Hedges, J. I., Keil, R. G., and Benner, R.: What happens to terrestrial organic matter in the ocean?, *Org. Geochem.*, 27, 195–212, 1997.

Higgins, M. B., Robinson, R. S., Carter, S. J., and Pearson, A.: Evidence from chlorin nitrogen isotopes for alternating nutrient regimes in the Eastern Mediterranean Sea, *Earth Planet. Sci. Lett.*, 290, 102–107, 2010.

Higgins, M. D., Robinson, R. S., Husson, J. M., Carter, S. J., and Pearson, A.: Dominant eukaryotic export production during ocean anoxic events reflects the importance of recycled NH_4^+ , *Proc. Nat. Acad. Sci. USA*, 109, 2269–2274, 2012.

Hoch, M. P., Fogel, M. L., and Kirchman, D. L.: Isotope fractionation during ammonium uptake by marine microbial assemblages, *Geomicrobiol. J.*, 12, 113–127, 1994.

Hollaway, J. M. and Dahlgren, R. A.: Geologic nitrogen in terrestrial biogeochemical cycling, *Geology*, 27, 567–570, 1999.

Icehouse-greenhouse variations in marine denitrification

T. J. Algeo et al.

[Title Page](#)[Abstract](#)[Introduction](#)[Conclusions](#)[References](#)[Tables](#)[Figures](#)[Back](#)[Close](#)[Full Screen / Esc](#)[Printer-friendly Version](#)[Interactive Discussion](#)

- Holloway, J. M., Dahlgren, R. A., Hansen, B., and Casey, W. H.: Contribution of bedrock nitrogen to high nitrate concentrations in stream water, *Nature*, 395, 785–788, 1998.
- Holmes, M. E., Eichner, C., Struck, U., and Wefer, G.: Reconstruction of surface ocean nitrate utilization using stable nitrogen isotopes in sinking particles and sediments, in: *Use of Proxies in Paleoceanography: Examples from the South Atlantic*, edited by: Fischer, G. and Wefer, G., Springer, Berlin, 447–468, 1999.
- Huang, W. Y. and Meinschein, W. G.: Sterols as ecological indicators, *Geochim. Cosmochim. Acta*, 43, 739–745, 1979.
- Hutton, A. C.: Petrographic classification of oil shales, *Internat. J. Coal Geol.*, 8, 203–231, 1987.
- Imbus, S. W., Macko, S. A., Elmore, R. D., and Engel, M. H.: Stable isotope (C, S, N) and molecular studies on the Precambrian Nonesuch Shale (Wisconsin-Michigan, USA): evidence for differential preservation rates, depositional environment and hydrothermal influence, *Chem. Geol.*, 101, 255–281, 1992.
- Jaminski, J., Algeo, T. J., Maynard, J. B., and Hower, J. C.: Climatic origin of dm-scale compositional cyclicity in the Cleveland Member of the Ohio Shale (Upper Devonian), Central Appalachian Basin, USA, in: Schieber, J., Zimmerle, W. and Sethi, P. S. (Eds.), *Shales and Mudstones*, v. 1, Schweizerbart'sche, Stuttgart, 217–242, 1998.
- Jenkyns, H. C., Gröcke, D. R., and Hesselbo, S. P.: Nitrogen isotope evidence for water mass denitrification during the early Toarcian (Jurassic) oceanic anoxic event, *Paleoceanography*, 16, 593–603, 2001.
- Jenkyns, H. C., Matthews, A., Tsikos, H., and Erel, Y.: Nitrate reduction, sulfate reduction, and sedimentary iron isotope evolution during the Cenomanian-Turonian oceanic anoxic event, *Paleoceanography*, 22, 1–17, 2007.
- Jia, Y. and Kerrich, R.: Nitrogen 15-enriched Precambrian kerogen and hydrothermal systems, *Geochem. Geophys. Geosyst.*, 5, 1–21, 2004.
- Junium, C. K. and Arthur, M. A.: Nitrogen cycling during the Cretaceous, Cenomanian-Turonian Oceanic Anoxic Event II, *Geochem. Geophys. Geosyst.*, 8, 1–18, 2007.
- Kenrick, P. and Crane, P. R.: The origin and early evolution of plants on land, *Nature*, 389, 33–39, 1997.
- Knapp, A. N., DiFiore, P. J., Deutsch, C., Sigman, D. M., and Lipschultz, F.: Nitrate isotopic composition between Bermuda and Puerto Rico: implications for N₂ fixation in the Atlantic Ocean, *Glob. Biogeochem. Cy.*, 22, 1–14, 2008.

Icehouse-greenhouse variations in marine denitrification

T. J. Algeo et al.

Title Page

Abstract

Introduction

Conclusions

References

Tables

Figures

◀

▶

◀

▶

Back

Close

Full Screen / Esc

Printer-friendly Version

Interactive Discussion



Kritee, K., Sigman, D. M., Granger, J., Ward, B. B., Jayakumar, A., and Deutsch, C.: Reduced isotope fractionation by denitrification under conditions relevant to the ocean, *Geochim. Cosmochim. Acta*, 92, 243–259, 2012.

Kuypers, M. M. M., Lavik, G., Woebken, D., Schmid, M., Fuchs, B. M., Amann, R., Jorgensen, B. B., and Jetten, M. S. M.: Massive nitrogen loss from the Benguela upwelling system through anaerobic ammonium oxidation, *Proc. Natl. Acad. Sci. USA*, 102, 6478–6483, 2005.

Lehmann, M. F., Sigman, D. M., and Berelson, W. M.: Coupling the N-15/N-14 and O-18/O-16 of nitrate as a constraint on benthic nitrogen cycling, *Mar. Chem.*, 88, 1–20, 2004.

Lehmann, M. F., Sigman, D. M., McCorkle, D. C., Granger, J., Hoffmann, S., Cane, G., and Brunelle, B. G.: The distribution of nitrate $^{15}\text{N}/^{14}\text{N}$ in marine sediments and the impact of benthic nitrogen loss on the isotopic composition of oceanic nitrate, *Geochim. Cosmochim. Acta*, 71, 5384–5404, 2007.

Libes, S. M. and Deuser, W. G.: The isotopic geochemistry of particulate nitrogen in the Peru Upwelling Area and the Gulf of Maine, *Deep-Sea Res. I*, 35, 517–533, 1988.

Liu, Z., Altabet, M. A., and Herbert, T. D.: Glacial-interglacial modulation of eastern tropical North Pacific denitrification over the last 1.8-Myr, *Geophys. Res. Lett.*, 32, 1–4, 2005.

Liu, Z., Altabet, M. A., and Herbert, T. D.: Plio-Pleistocene denitrification in the eastern tropical North Pacific: intensification at 2.1 Ma, *Geochem. Geophys. Geosyst.*, 9, 1–14, 2008.

Lourey, M. J., Trull, T. W., and Sigman, D. M.: Sensitivity of $\delta^{15}\text{N}$ of nitrate, surface suspended and deep sinking particulate nitrogen to seasonal nitrate depletion in the Southern Ocean, *Glob. Biogeochem. Cy.*, 17, 1081, 1–18, 2003.

Lücke, A. and Brauer, A.: Biogeochemical and micro-facial fingerprints of ecosystem response to rapid Late Glacial climatic changes in varved sediments of Meerfelder Maar (Germany), *Palaeogeogr. Palaeoclimatol. Palaeoecol.*, 211, 139–155, 2004.

Luo, G., Wang, Y., Kump, L. R., Bai, X., Algeo, T. J., Yang, H., and Xie, S.: Enhanced nitrogen fixation in the aftermath of the latest Permian marine mass extinction, *Geology*, 39, 647–650, 2011.

Macko, S. A. and Estep, M. L. F.: Microbial alteration of stable nitrogen and carbon isotopic compositions of organic matter, *Org. Geochem.*, 6, 787–790, 1984.

Macko, S. A., Estep, M. L. F., Engel, M. H., and Hare, P. E.: Kinetic fractionation of stable nitrogen isotopes during amino acid transamination, *Geochim. Cosmochim. Acta*, 50, 2143–2146, 1986.

Icehouse-greenhouse variations in marine denitrification

T. J. Algeo et al.

Title Page

Abstract

Introduction

Conclusions

References

Tables

Figures

◀

▶

◀

▶

Back

Close

Full Screen / Esc

Printer-friendly Version

Interactive Discussion



- Macko, S. A., Fogel, M. L., Hare, P. E., and Hoering, T. C.: Isotopic fractionation of nitrogen and carbon in the synthesis of amino acids by microorganisms, *Chem. Geol.*, 65, 79–92, 1987.
- MacLeod, K. G. and Huber, B. T.: Reorganization of deep ocean circulation accompanying a Late Cretaceous extinction event, *Nature*, 380, 422–425, 1996.
- 5 Mariotti, A.: Natural ^{15}N abundance measurements and atmospheric nitrogen standard calibration, *Nature*, 311, 251–252, 1984.
- Meyers, P. A.: Preservation of elemental and isotopic source identification of sedimentary organic matter, *Chem. Geol.*, 114, 289–302, 1994.
- Meyers, P. A.: Organic geochemical proxies of paleoceanographic, paleolimnologic, and paleo-
- 10 climatic processes, *Org. Geochem.*, 27, 213–250, 1997.
- Meyers, P. A., Yum, J.-G., and Wise, S. W.: Origins and maturity of organic matter in mid-Cretaceous black shales from ODP Site 1138 on the Kerguelen Plateau, *Mar. Petrol. Geol.*, 26, 909–915, 2009a.
- Meyers, P. A., Bernasconi, S. M., and Yum, J.-G.: 20 My of nitrogen fixation during deposition of mid-Cretaceous black shales on the Demerara Rise, equatorial Atlantic Ocean, *Org. Geochem.*, 40, 158–166, 2009b.
- Middelburg, J. J., Soetaert, K., Herman, P. M. J., and Heip, C. H. R.: Denitrification in marine sediments: a model study, *Glob. Biogeochem. Cycles*, 10, 661–673, 1996.
- Mii, H.-S., Grossman, E. L., Yancey, T. E., Chuvashov, B., and Egorov, A.: Isotopic records fo
- 20 brachiopod shells from the Russian Platform – evidence for the onset of mid-Carboniferous glaciation, *Chem. Geol.*, 175, 133–147, 2001.
- Montañez, I. P. and the Committee on the Importance of Deep-Time Geologic Records for Understanding Climate Change Impacts: Understanding Earth's Deep Past: Lessons for Our Climate Future, National Academy of Sciences, Washington, DC, 212 pp., 2011.
- 25 Mulder, A., van de Graaf, A. A., Robertson, L. A., and Kuenen, J. G.: Anaerobic ammonium oxidation discovered in a denitrifying fluidized bed reactor, *FEMS Microbiol. Ecol.*, 16, 177–184, 1995.
- Müller, P. J.: C/N ratios in Pacific deep-sea sediments: Effect of inorganic ammonium and organic nitrogen compounds sorbed by clays, *Geochim. Cosmochim. Acta*, 41, 765–776, 1977.
- 30 Murray, J. W., Fuchsman, C., Kirkpatrick, J., Paul, B., and Konovalov, S. K.: Species and $\delta^{15}\text{N}$ signatures of nitrogen transformations in the suboxic zone of the Black Sea, *Oceanography*, 18, 36–47, 2005.

Icehouse-greenhouse variations in marine denitrification

T. J. Algeo et al.

Title Page

Abstract

Introduction

Conclusions

References

Tables

Figures

◀

▶

◀

▶

Back

Close

Full Screen / Esc

Printer-friendly Version

Interactive Discussion



- Naqvi, S. W. A., Yoshinari, T., Jayakumar, D. A., Altabet, M. A., Narvekar, P. V., Devol, A. H., Brandes, J. A., and Codispoti, L. A.: Budgetary and biogeochemical implications of N_2O isotope signatures in the Arabian Sea, *Nature*, 394, 462–464, 1998 .
- Ogrinc, N., Fontolan, G., Faganeli, J., and Covelli, S.: Carbon and nitrogen isotope compositions of organic matter in coastal marine sediments (the Gulf of Trieste, N Adriatic Sea): indicators of sources and preservation, *Mar. Chem.*, 95, 163–181, 2005.
- Peters, K. E.: Guidelines for evaluating petroleum source rock using programmed pyrolysis, *Am. Assoc. Petrol. Geol. Bull.*, 70, 318–329, 1986.
- Peters, K. E., Walters, C. C., and Moldowan, J. M., *The Biomarker Guide*, 2nd Edn., Vol. 2 , Cambridge University Press, Cambridge, 2004.
- Prahl, F. G., de Lange, G. J., Scholten, S., and Cowie, G. L.: A case of post-depositional aerobic degradation of terrestrial organic matter in turbidite deposits from the Madeira abyssal plain, *Org. Geochem.*, 27, 141–152, 1997.
- Prokopenko, M. G., Hammond, D. E., Berelson, W. M., Bernhard, J. M., Stott, L., and Douglas, R.: Nitrogen cycling in the sediments of Santa Barbara basin and Eastern Subtropical North Pacific: nitrogen isotopes, diagenesis and possible chemosymbiosis between two lithotrophs (*Thioploca* and *Anammox*) – “riding on a glider”, *Earth Planet. Sci. Lett.*, 242, 186–204, 2006.
- Rau, G. H., Arthur, M. A., and Dean, W. E.: $^{15}N/^{14}N$ variations in Cretaceous Atlantic sedimentary sequences: Implication for past changes in marine nitrogen biogeochemistry, *Earth Planet. Sci. Lett.*, 82, 269–279, 1987.
- Robinson, R. S. and Meyers, P. A.: Biogeochemical changes within the Benguela Current upwelling system during the Matuyama Diatom Maximum: Nitrogen isotope evidence from Ocean Drilling Program Sites 1082 and 1084, *Paleoceanography*, 17, 1–10, 2002.
- Robinson, R. S., Sigman, D. M., DiFiore, P. J., Rohde, M. M., Mashiotta, T. A., and Lea, D. W.: Diatom-bound $^{15}N/^{14}N$: New support for enhanced nutrient consumption in the ice age subantarctic, *Paleoceanography*, 20, 1–14, 2005.
- Robinson, R. S. et al.: A review of nitrogen isotope alteration in marine sediments, *Paleoceanography*, 27, 1–13, 2012.
- Romano, C., Goudemand, N., Vennemann, T. W., Ware, D., Schneebeli-Hermann, E., Hochuli, P. A., Brühwiler, T., Brinkmann, W., and Bucher, H.: Climatic and biotic upheavals following the end-Permian mass extinction, *Nat. Geosci.*, 6, 57–60, 2012.

Icehouse-greenhouse variations in marine denitrification

T. J. Algeo et al.

[Title Page](#)[Abstract](#)[Introduction](#)[Conclusions](#)[References](#)[Tables](#)[Figures](#)[⏪](#)[⏩](#)[◀](#)[▶](#)[Back](#)[Close](#)[Full Screen / Esc](#)[Printer-friendly Version](#)[Interactive Discussion](#)

- Sachs, J. P. and Repeta, D. J.: Oligotrophy and nitrogen fixation during Eastern Mediterranean sapropel events, *Science*, 286, 2485–2488, 1999.
- Sachs, J. P., Repeta, D. J., and Goericke, R.: Nitrogen and carbon isotopic ratios of chlorophyll from marine phytoplankton, *Geochim. Cosmochim. Acta*, 63, 1431–1441, 1999.
- 5 Saino, T.: ^{15}N and ^{13}C natural abundance in suspended particulate organic matter from a Kuroshio warm-core ring, *Deep-Sea Res. I*, 39, 347–362, 1992.
- Saltzman, M. R.: Late Paleozoic ice age: oceanic gateway or $p\text{CO}_2?$, *Geology*, 31, 151–154, 2003.
- Schoepfer, S. D., Henderson, C. M., Garrison, G. H., and Ward, P. D.: Cessation of a productive coastal upwelling system in the Panthalassic Ocean at the Permian-Triassic boundary, *Palaeogeogr. Palaeoclimatol. Palaeoecol.*, 313/314, 181–188, 2012.
- 10 Schoepfer, S. D., Henderson, C. M., Garrison, G. H., Ward, P. D., Foriel, J., Selby, D., Hower, J. C., Algeo, T. J., and Shen, Y.: Termination of a continent-margin upwelling system at the Permian-Triassic boundary (Opal Creek, Alberta, Canada), *Glob. Planet. Change*, 105, 21–35, 2013.
- 15 Sephton, M. A., Looy, C. V., Brinkhuis, H., Wignall, P. B., de Leeuw, J. W., and Visscher, H.: Catastrophic soil erosion during the end-Permian biotic crisis, *Geology*, 33, 941–944, 2005.
- Sigman, D. M., Altabet, M. A., François, R., McCorkle, D. C., and Gaillard, J.-F.: The isotopic composition of diatom-bound nitrogen in Southern Ocean sediments, *Paleoceanography*, 14, 118–134, 1999.
- 20 Sigman, D. M., Altabet, M. A., McCorkle, D. C., François, R., and Fischer, G.: The $\delta^{15}\text{N}$ of nitrate in the Southern Ocean: nitrogen cycling and circulation in the ocean interior, *J. Geophys. Res.*, 105, 19599–19614, 2000.
- Sigman, D. M., Robinson, R., Knapp, A. N., van Geen, A., McCorkle, D. C., Brandes, J. A., and Thunell, R. C.: Distinguishing between water column and sedimentary denitrification in the Santa Barbara Basin using the stable isotopes of nitrate, *Geochem. Geophys. Geosyst.*, 4, 1040, 1–20, 2003.
- 25 Somes, C. J., Schmittner, A., and Altabet, M. A.: Nitrogen isotope simulations show the importance of atmospheric iron deposition for nitrogen fixation across the Pacific Ocean, *Geophys. Res. Lett.*, 37, 1–6, 2010.
- 30 Song, H. Y., Tong, J. N., Algeo, T. J., Horacek, M., Qiu, H. O., Song, H. J., Tian, L., and Chen, Z. Q.: Large vertical $\delta^{13}\text{C}$ gradients in Early Triassic seas of the South China craton: Implica-

tions for oceanographic changes related to Siberian Traps volcanism, *Glob. Planet. Change*, 105, 7–20, 2013.

Sun, Y., Joachimski, M. M., Wignall, P. B., Yan, C., Chen, Y., Jiang, H., Wang, L., and Lai, X.: Lethally hot temperatures during the Early Triassic greenhouse, *Science*, 338, 366–370, 2012.

Suthhof, A., Ittekkot, V., and Gaye-Haake, B.: Millennial-scale oscillation of denitrification intensity in the Arabian Sea during the late Quaternary and its potential influence on atmospheric N₂O and global climate, *Glob. Biogeochem. Cycles*, 15, 637–649, 2001.

Tesdal, J.-E., Galbraith, E. D., and Kienast, M.: Nitrogen isotopes in bulk marine sediment: linking seafloor observations with subseafloor records, *Biogeosciences*, 10, 101–118, doi:10.5194/bg-10-101-2013, 2013.

Thamdrup, B., Dalsgaard, T., Jensen, M. M., Ulloa, O., Farías, L., and Escribano, R.: Anaerobic ammonium oxidation in the oxygen-deficient waters off northern Chile, *Limnol. Oceanogr.*, 51, 2145–2156, 2006.

Thornton, S. F. and McManus, J.: Application of organic carbon and nitrogen stable isotopes and OC/TN ratios as source indicators of OM provenance in estuarine systems: evidence from the Tay Estuary, Scotland, *Estuar. Coast. Shelf Sci.*, 38, 219–233, 1994.

Tyrrell, T.: The relative influences of nitrogen and phosphorus on oceanic primary productivity, *Nature*, 400, 525–531, 1999.

Voss, M., Dippner, J. W., and Montoya, J. P.: Nitrogen isotope patterns in the oxygen-deficient waters of the Eastern Tropical North Pacific Ocean, *Deep-Sea Res. I*, 48, 1905–1921, 2001.

Wang, C. J. and Visscher, H.: Abundance anomalies of aromatic biomarkers in the Permian-Triassic boundary section at Meishan, China—Evidence of end-Permian terrestrial ecosystem collapse, *Palaeogeogr. Palaeoclimatol. Palaeoecol.*, 252, 291–303, 2007.

Waser, N. A. D., Harrison, P. J., Nielsen, B., Calvert, S. E., and Turpin, D. H.: Nitrogen isotope fractionation during the uptake and assimilation of nitrate, nitrite, ammonium and urea by a marine diatom, *Limnol. Oceanogr.*, 43, 215–224, 1998.

Xie, S., Pancost, R. D., Huang, J., Wignall, P. B., Yu, J., Tang, X., Chen, L., Huang, X., and Lai, X.: Changes in the global carbon cycle occurred as two episodes during the Permian-Triassic crisis, *Geology*, 35, 1083–1086, 2007.

BGD

10, 14769–14813, 2013

Icehouse-greenhouse variations in marine denitrification

T. J. Algeo et al.

Title Page

Abstract

Introduction

Conclusions

References

Tables

Figures

◀

▶

◀

▶

Back

Close

Full Screen / Esc

Printer-friendly Version

Interactive Discussion



Icehouse-greenhouse variations in marine denitrification

T. J. Algeo et al.

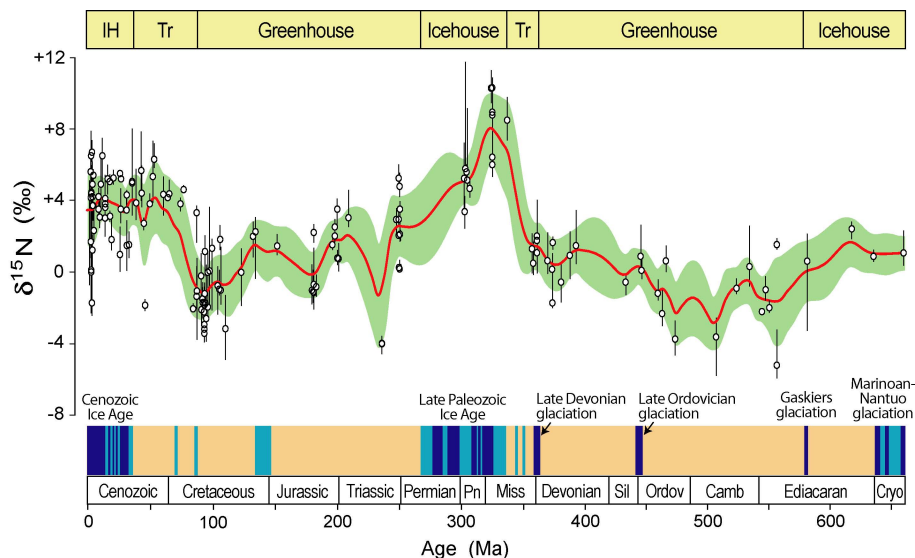


Fig. 1. Mean $\delta^{15}\text{N}$ for 153 marine sedimentary units of Vendian to Recent age. This dataset yields a Phanerozoic-mean $\delta^{15}\text{N}_{\text{sed}}$ of $+2.0 \pm 0.3\text{‰}$ (mean ± 1 standard error of the mean). For each unit, the distribution of $\delta^{15}\text{N}$ values is represented by the median (open circle) and the 16th-to-84th percentile range (vertical line) (see Supplement Table 1). The long-term trend is shown by a LOWESS curve (red curve) and standard deviation envelope ($\pm 1\sigma$; green field). Note variation of the LOWESS curve over a $\sim 10\text{‰}$ range, accounting for 74 % of total variance in the $\delta^{15}\text{N}_{\text{sed}}$ dataset. Shown at bottom is the 2012 geologic timescale (Gradstein et al., 2012) and intervals of moderate (light blue) and heavy (dark blue) continental glaciation (Montañez et al., 2011). IH = icehouse, Tr = transitional.

Title Page

Abstract

Introduction

Conclusions

References

Tables

Figures



Back

Close

Full Screen / Esc

Printer-friendly Version

Interactive Discussion

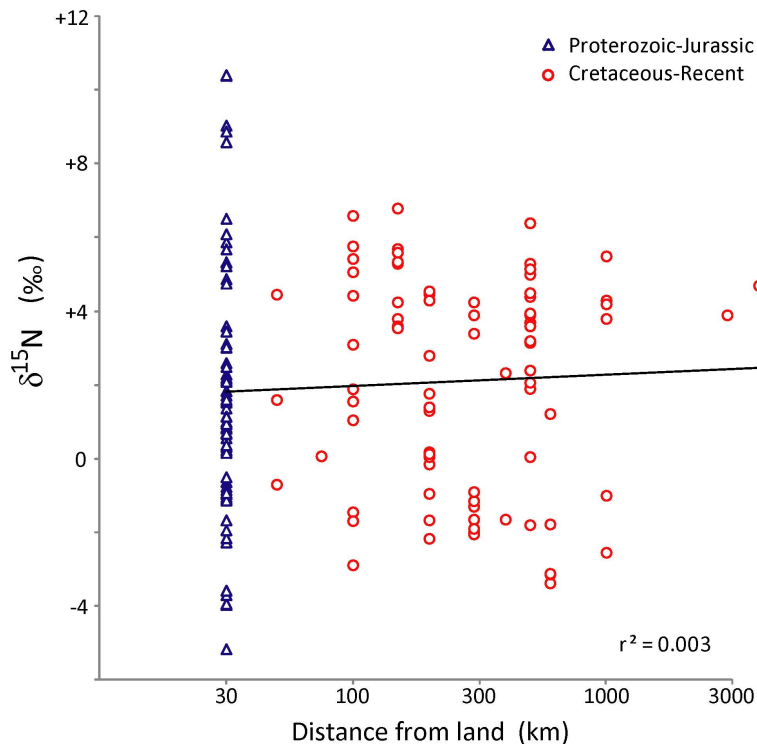


Fig. 2. Mean $\delta^{15}\text{N}_{\text{sed}}$ versus distance from land. All Proterozoic to Jurassic units were arbitrarily plotted at a distance of 30 km owing to their epicontinental settings and uncertainties regarding paleocoastal geography. Distances for Cretaceous to Recent units were measured from the paleogeographic map series of Ron Blakey (Colorado Plateau Geosystems, <http://cpgeosystems.com/>). Note the lack of any relationship between $\delta^{15}\text{N}$ and the distance of the depositional site from land.

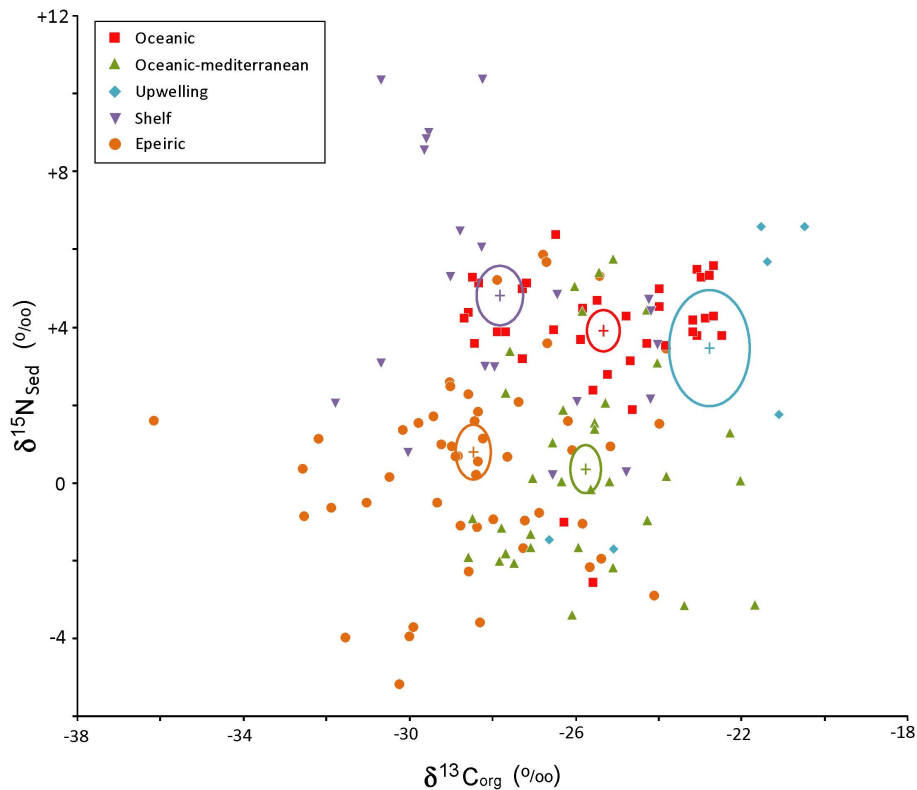


Fig. 3. $\delta^{15}\text{N}_{\text{sed}}$ versus $\delta^{13}\text{C}_{\text{org}}$ for 153 Phanerozoic marine units. The average $\delta^{15}\text{N}_{\text{sed}}-\delta^{13}\text{C}_{\text{org}}$ compositions for five depositional settings are shown by crosses (mean) and ovals (one standard error of the mean). The dataset as a whole exhibits no significant covariation between $\delta^{15}\text{N}_{\text{sed}}$ and $\delta^{13}\text{C}_{\text{org}}$. However, there are statistically significant differences in average $\delta^{15}\text{N}_{\text{sed}}-\delta^{13}\text{C}_{\text{org}}$ compositions by depositional setting (see Sect. 4.4 and Fig. 5).

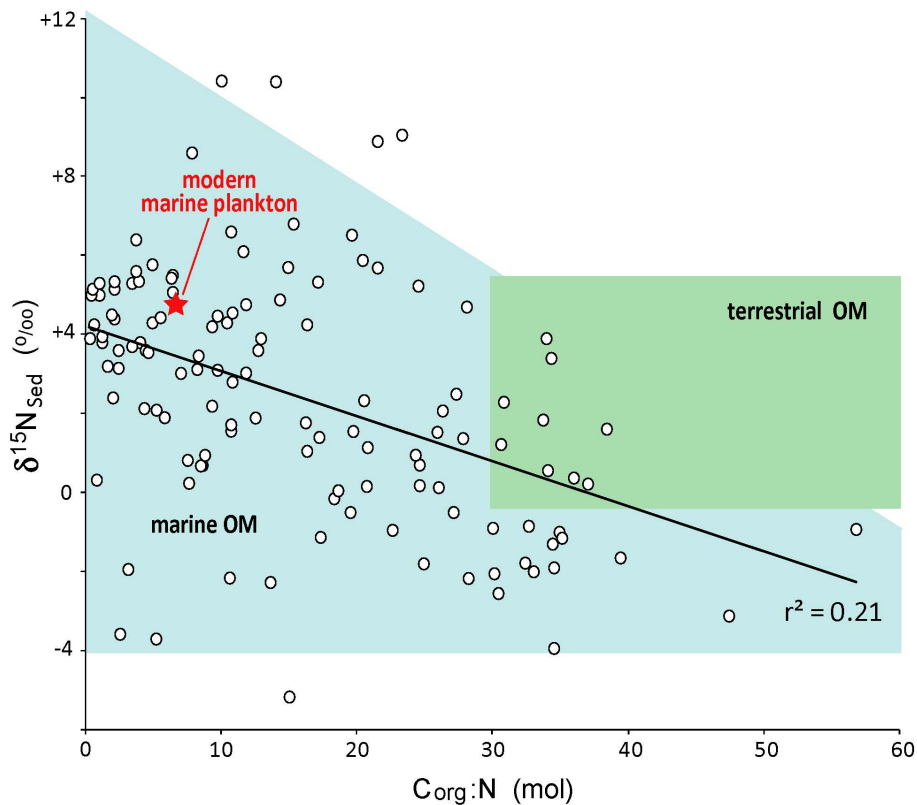


Fig. 4. $\delta^{15}\text{N}_{\text{sed}}$ versus $\text{C}_{\text{org}}:\text{N}$ ratio. Average composition of modern marine plankton shown by red star, and approximate compositional range of terrestrial (i.e., soil-derived) organic matter by green rectangle. Note that the pattern of negative covariation between $\delta^{15}\text{N}_{\text{sed}}$ and $\text{C}_{\text{org}}:\text{N}$ is not clearly associated with a terrestrial endmember and does not provide evidence of pervasive mixing of marine and terrestrial organic matter in our study units.

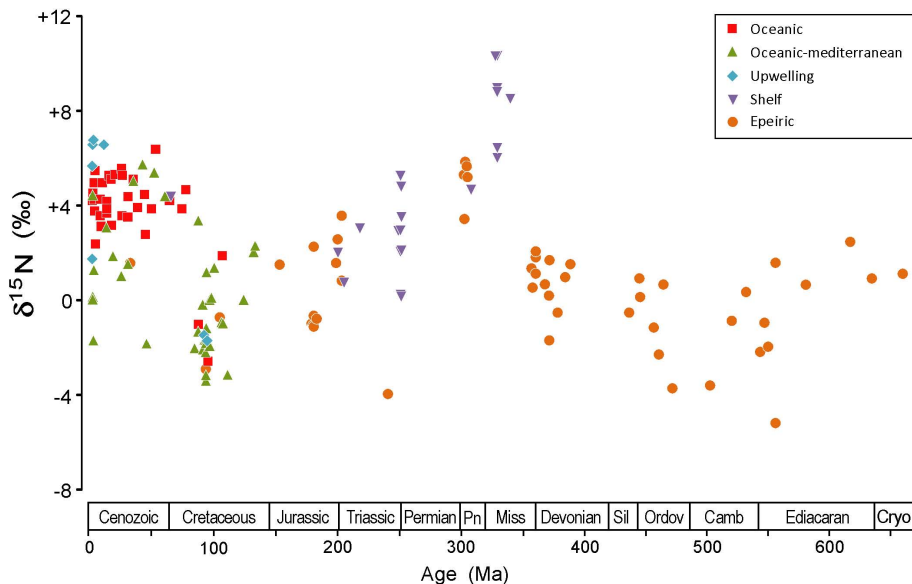


Fig. 5. $\delta^{15}\text{N}_{\text{sed}}$ as a function of depositional setting. For the Neogene, upwelling units are 1.3 ‰ enriched and oceanic-mediterranean units 3.0 ‰ depleted in ^{15}N on average relative to oceanic units. For units of any given age, note the generally limited variation in $\delta^{15}\text{N}_{\text{sed}}$ among different setting types, relative to the larger variation in $\delta^{15}\text{N}_{\text{sed}}$ through time. For the Phanerozoic as a whole, note the smooth $\delta^{15}\text{N}_{\text{sed}}$ transition in the mid-Mesozoic between entirely different setting types, i.e., epeiric and shelf in the Jurassic and earlier versus mainly oceanic and oceanic-mediterranean in the Cretaceous and later.

Icehouse-greenhouse variations in marine denitrification

T. J. Algeo et al.

Title Page

Abstract Introduction

Conclusions References

Tables Figures

◀ ▶

◀ ▶

Back Close

Full Screen / Esc

Printer-friendly Version

Interactive Discussion



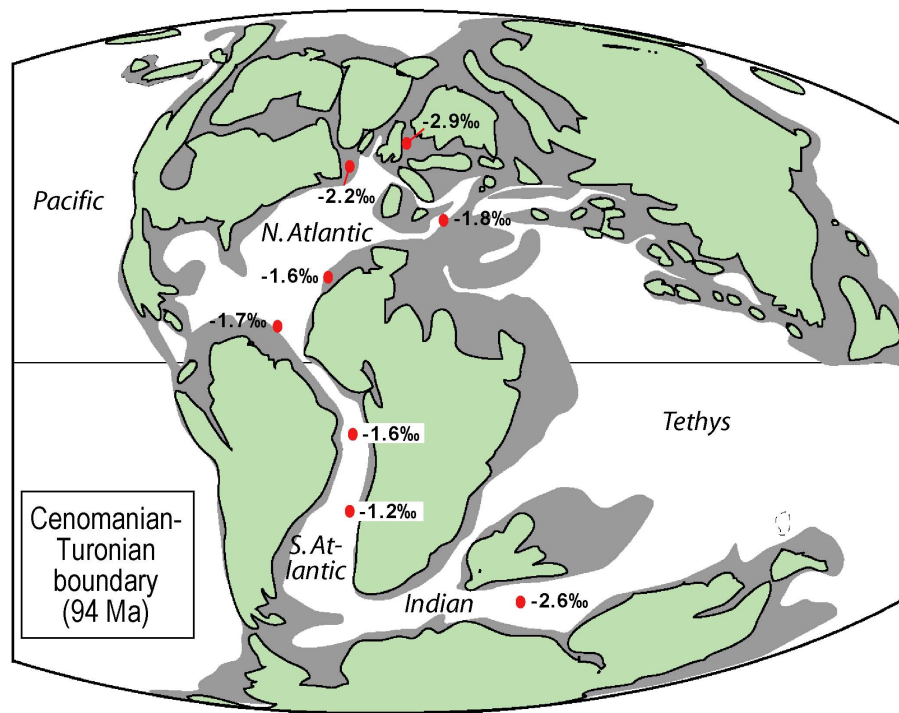


Fig. 6. Average $\delta^{15}\text{N}_{\text{sed}}$ for Cenomanian-Turonian boundary units. Note the limited range of $\delta^{15}\text{N}_{\text{sed}}$ values (-2.9 to -1.2 ‰) for sites ranging from high northern to high southern paleo-latitudes, implying a relatively uniform contemporaneous seawater $\delta^{15}\text{N}_{\text{NO}_3^-}$ composition. Data sources in Supplement Table 1.

Icehouse-greenhouse variations in marine denitrification

T. J. Algeo et al.

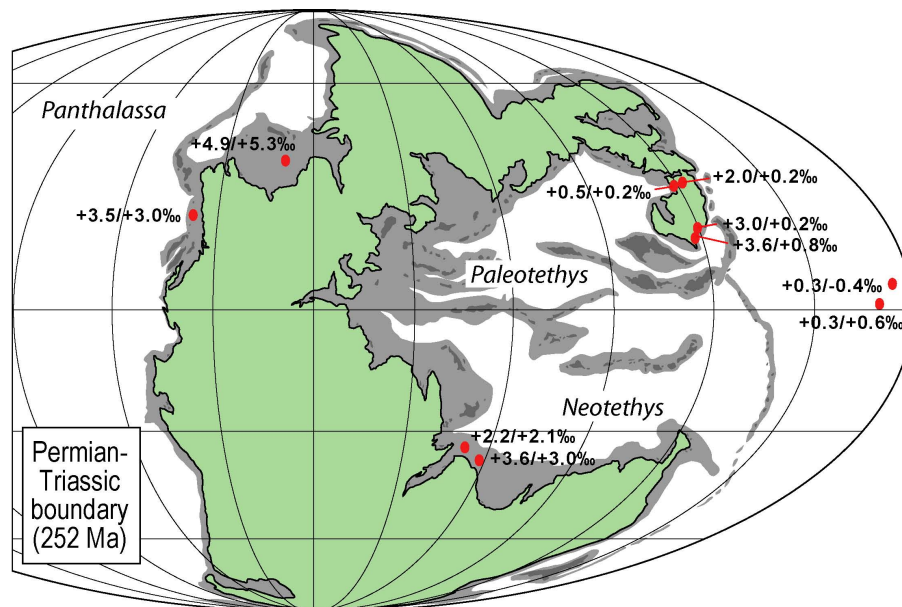


Fig. 7. Average $\delta^{15}\text{N}_{\text{sed}}$ for Upper Permian (left) and Lower Triassic (right) units. Upper Permian $\delta^{15}\text{N}_{\text{sed}}$ varies from low values in the central Panthalassic Ocean (+0.3‰) to intermediate values in the Tethyan region and high values on the northwestern Pangean margin (+4.9‰), probably owing to higher rates of water-column denitrification in the latter regions. Note that all Permo-Triassic $\delta^{15}\text{N}_{\text{sed}}$ values globally are intermediate relative to the low values characteristic of the CTB or the high values characteristic of the Carboniferous (Fig. 1). Site-specific changes in $\delta^{15}\text{N}_{\text{sed}}$ across the PTB range from -2.8 to $+0.4$ ‰ with an average of -0.9 ‰, which is consistent with our hypothesis of intensified sedimentary denitrification during greenhouse climate intervals such as the Early Triassic. Data sources in Supplement Table 1 with additional data from S. Schoepfer and T. Algeo (unpublished data).

Title Page

Abstract

Introduction

Conclusions

References

Tables

Figures

◀

▶

◀

▶

Back

Close

Full Screen / Esc

Printer-friendly Version

Interactive Discussion



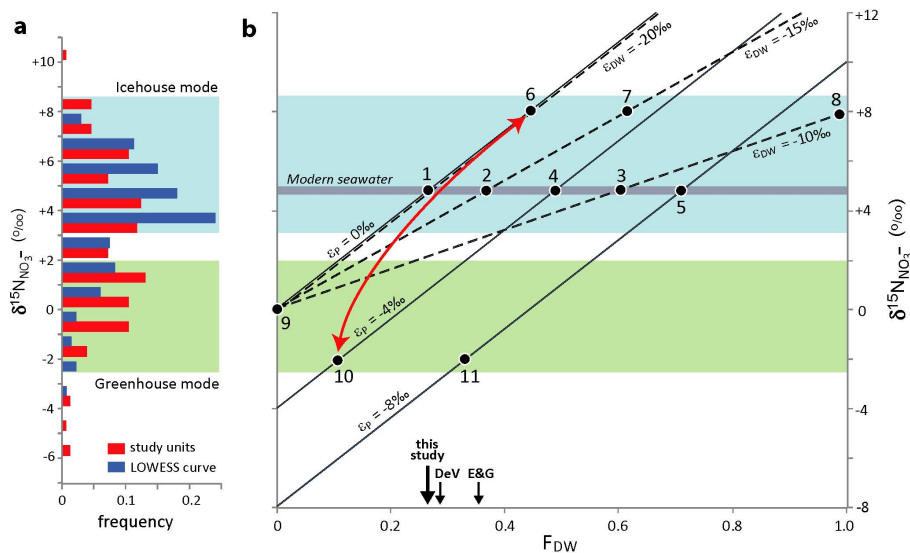


Fig. 8. $\delta^{15}\text{N}$ distributions and modeling constraints. **(a)** Frequency distributions for unit-median $\delta^{15}\text{N}_{\text{sed}}$ values (red) and LOWESS curve values (blue). Note that both distributions exhibit bimodal character, with modes at ~ -2 to $+2$ ‰ and $\sim +4$ to $+8$ ‰ representative of greenhouse and icehouse climate modes, respectively. **(b)** Reservoir box model estimates of $\delta^{15}\text{N}_{\text{NO}_3^-}$ as a function of the fraction of water-column denitrification (F_{DW}). The dashed diagonal lines represent variable fractionation during water column-denitrification (ϵ_{DW}), and the solid diagonal lines variable fractionation during photosynthetic uptake of seawater fixed N (ϵ_{P}). Colored fields show the isotopic range of marine $\delta^{15}\text{N}_{\text{sed}}$ during greenhouse (green) and icehouse (blue) climate modes as well as modern seawater $\delta^{15}\text{N}_{\text{NO}_3^-}$ (gray) (Sigman et al., 2000). Arrows at bottom show F_{DW} of 0.27 (this study), 0.29 (DeVries et al., 2012), and 0.36 (Eugster and Gruber, 2012). The red curve represents our “most likely scenario” of concurrent changes in F_{DW} and ϵ_{P} as a function of greenhouse-icehouse climate shifts. See text for discussion of numbered points.

Title Page

Abstract

Introduction

Conclusions

References

Tables

Figures

◀

▶

◀

▶

Back

Close

Full Screen / Esc

Printer-friendly Version

Interactive Discussion



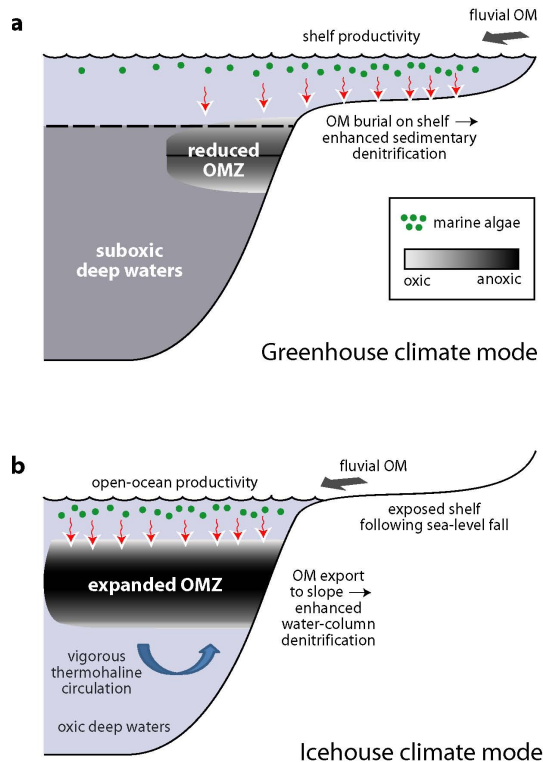


Fig. 9. Model for eustatic control of long-term $\delta^{15}\text{N}_{\text{sed}}$ variation. **(a)** Greenhouse climate mode. High eustatic levels result in on-shelf marine productivity and delivery of fluvial organic matter (OM) to shelf environments. Large quantities of OM are trapped in shelf sediments, enhancing sedimentary denitrification. **(b)** Icehouse climate mode. Low eustatic levels result in open-ocean productivity and delivery of fluvial OM to shelf margins. The sinking flux of OM to the thermocline is elevated, leading to expansion of the oxygen-minimum zone (OMZ) and enhanced water-column denitrification.

Icehouse-greenhouse variations in marine denitrification

T. J. Algeo et al.

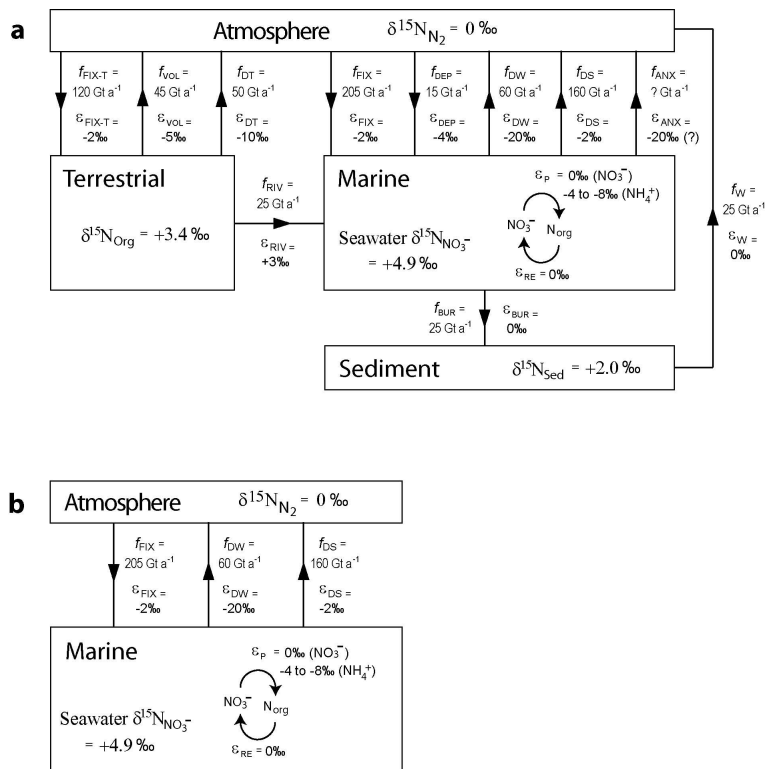


Fig. C1. Marine nitrogen cycle models. **(a)** Fully integrated marine-terrestrial-atmosphere N cycle. **(b)** Simplified N cycle model, which is limited to the most important source flux (cyanobacterial N fixation) and sink fluxes (sedimentary and water-column denitrification) of seawater fixed N. Fluxes (f) and fractionation factors (ε) are shown for cyanobacterial fixation (FIX), soil volatilization (VOL), terrestrial denitrification (DT), riverine transport (RIV), atmospheric deposition (DEP), water-column denitrification (DW), sedimentary denitrification (DS), the anammox process (ANX), organic burial (BUR), sedimentary ammonification (AMM), and weathering (W). Sources of model parameters and discussion of model output are given in the text.

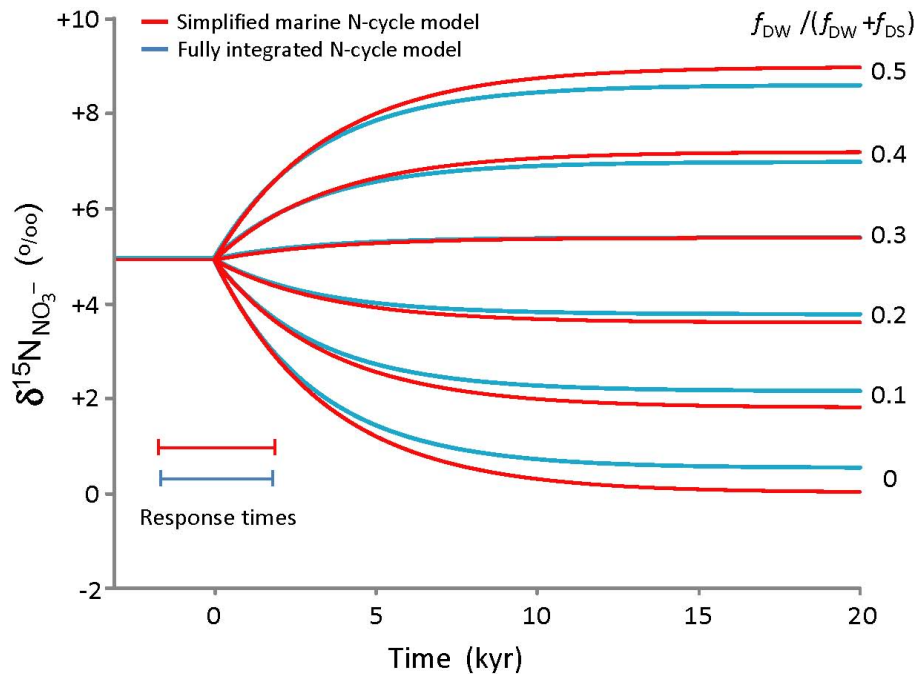


Fig. C2. Comparison of output of fully integrated and simplified N cycle models. At $t < 0$, the model is at equilibrium and represents our “baseline” scenario ($f_{\text{FIX}} = 220 \text{ Tg a}^{-1}$, $f_{\text{DW}} = 60 \text{ Tg a}^{-1}$, $f_{\text{DS}} = 160 \text{ Tg a}^{-1}$, $\epsilon_{\text{FIX}} = -2\%$, $\epsilon_{\text{DS}} = -2\%$, $\epsilon_{\text{DW}} = -20\%$, $\epsilon_{\text{P}} = 0\%$, and $F_{\text{DW}} = 0.27$), which yields a seawater $\delta^{15}\text{N}_{\text{NO}_3^-}$ value of $+4.9\%$ (i.e., equivalent to modern seawater nitrate; Sigman et al., 2000). At $t = 0$, changes in FDW to values ranging from 0 to 0.5 result in evolution of $\delta^{15}\text{N}_{\text{NO}_3^-}$ at a rate reflecting the response time of the system (which is closely related to the 3 kyr residence time of nitrate in seawater; Tyrrell, 1999; Brandes and Devol, 2002). Differences in $\delta^{15}\text{N}_{\text{NO}_3^-}$ between the fully integrated model (blue curves) and simplified model (red curves) are generally $< 0.4\%$, indicating that the output of the simplified model is robust.